

UNDERSTANDING THE ORIGIN OF MOLECULAR CHIRALITY

Cornelia MEINERT

Institut de Chimie de Nice (ICN), CNRS UMR 7272

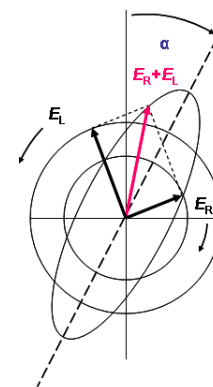
Université de Nice Sophia Antipolis

 @ConnyCNRS

Séminaire Laboratoire Leprince-Ringuet

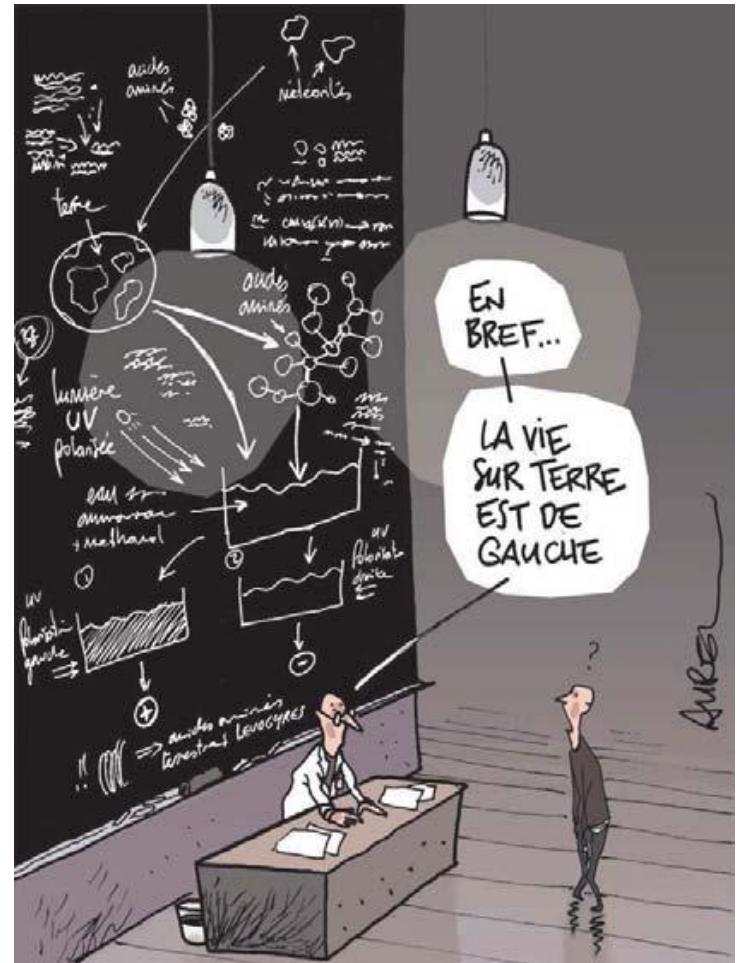
Ecole Polytechnique

Paris: 24.10.2016



How did life originate ?

And why were left-handed amino acids
& right-handed sugars selected for its
architecture ?



« La lumière a donné un sens à la vie »
Le Monde: 08-01-2011

BUILDING BLOCKS OF LIFE: WHERE DO THEY COME FROM?

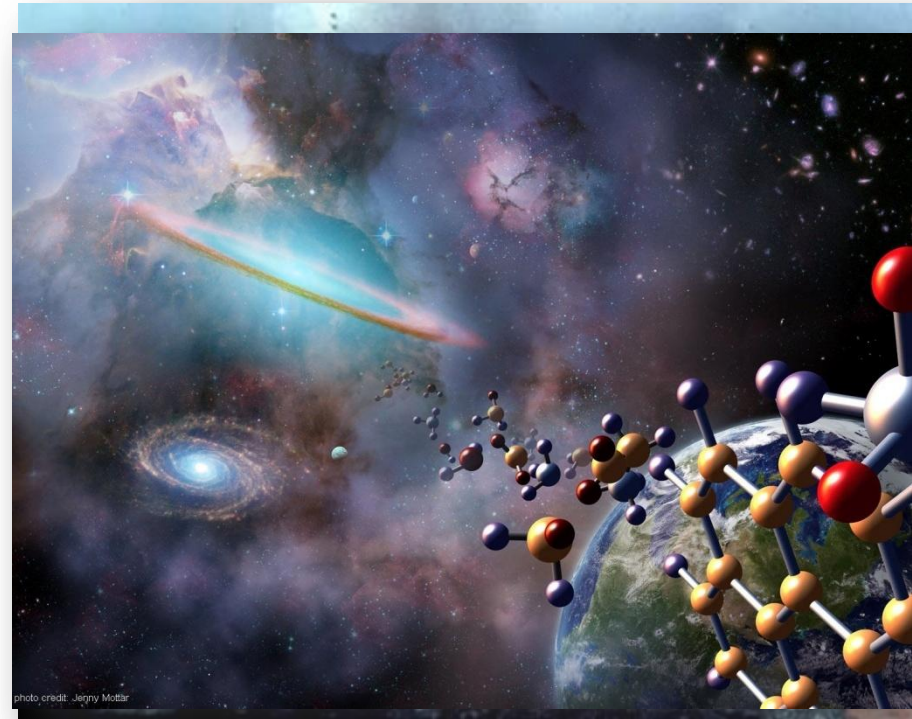
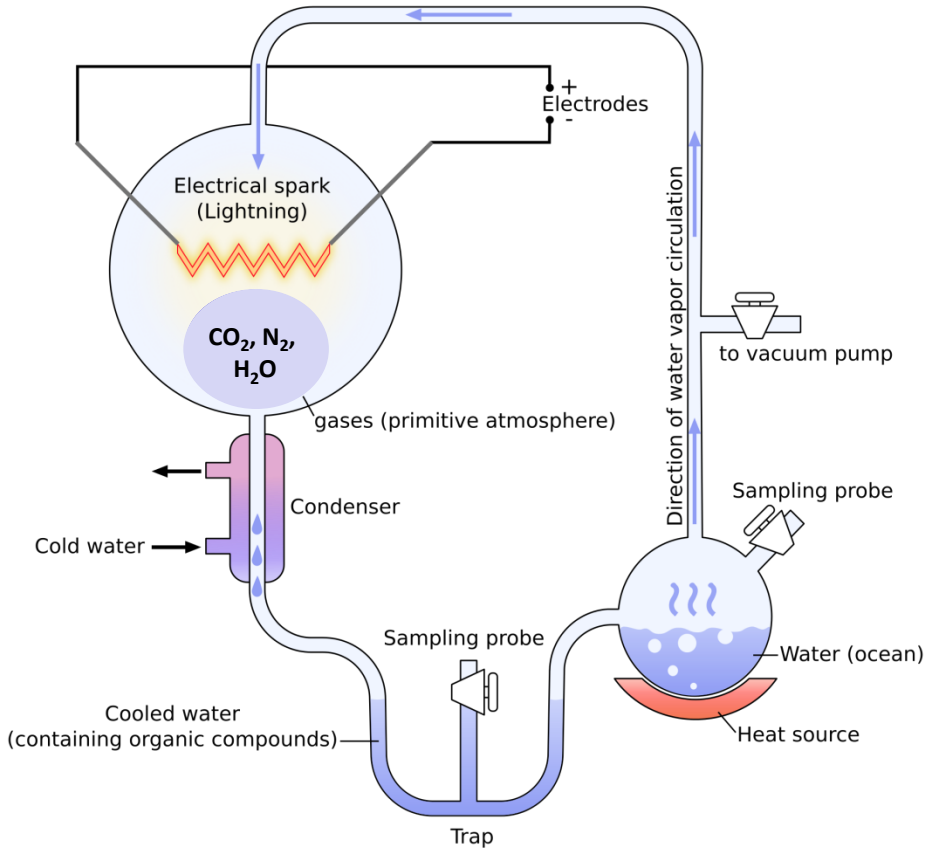
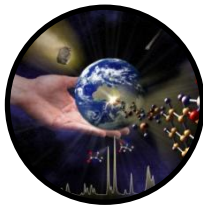


Fig. 1 Schematic set-up of Miller-Urey experiment.

Miller & Urey. *Science* **117**, 528 (1953).



Fig. 2: The Orion nebula - a happening place where stars are born - is stirring up the cosmic scene in this picture from NASA's Spitzer Space Telescope (Jan 2010). The hottest stars in the region, called the Trapezium cluster, are bright spots at center right. Radiation and winds from those stars has sculpted and blown away surrounding dust. The densest parts of the cloud appear dark at center left.

ORIGINS OF INTERSTELLAR BIOMOLECULES – INSIGHTS FROM COMETARY AND METEORITIC MATTER

Total carbon 2 %

Over 500 organic compounds

Aliphatic hydrocarbons	> 10 ppm
Aromatic hydrocarbons	> 10 ppm
Polar hydrocarbons	> 100 ppm
Volatile hydrocarbons	> 1 ppm
Aldehydes and ketones	> 10 ppm
Alcohols	> 10 ppm
Amines	> 1 ppm
Monocarboxylic acids	> 100 ppm
Dicarboxylic acids	> 10 ppm
Sulfonic acids	> 100 ppm
Phosphonic acids	> 1 ppm
N-heterocycles	> 1 ppm
Purines & Pyrimidines	> 1 ppm
Carboxamides	> 10 ppm
Hydroxy acids	> 10 ppm
Amino acids	> 10 ppm

Cronin J.R.: Clues from the origin of the Solar System: meteorites. In: Brack, A., The Molecular Origins of Life. Cambridge University Press 1998, pp. 119-146.



Fig. 3: Fragment of the Murchison Meteorite – CM2-type carbonaceous chondrite)



...more than 90 amino acids
identified in Murchison meteorite!

MULTIDIMENSIONAL ENANTIOSELECTIVE GAS CHROMATOGRAPHY

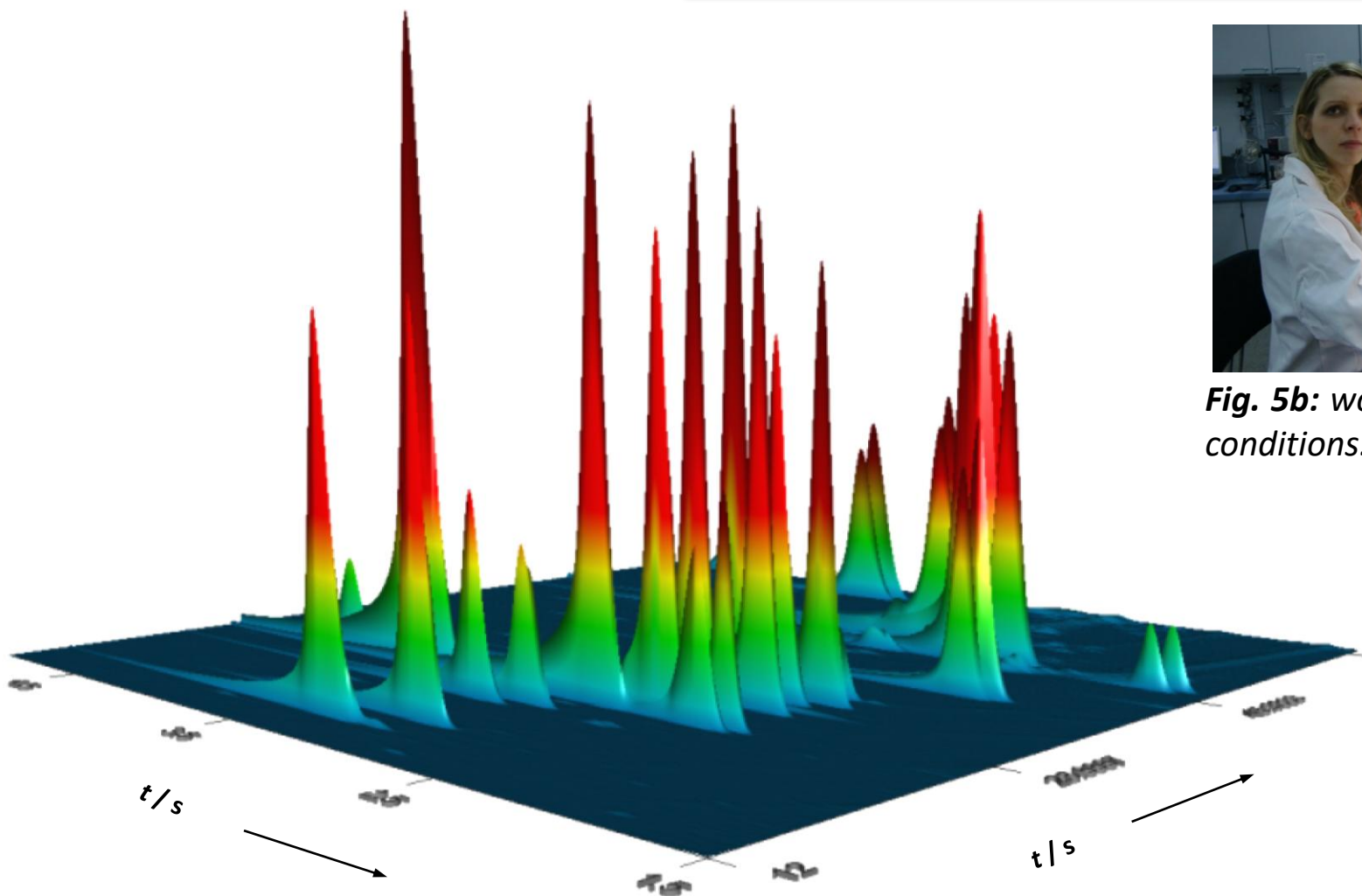


Fig. 5a: Amino acid separation using enantioselective multidimensional gas chromatography after derivatization as N-ethoxycarbonyl heptafluorobutanol ester.

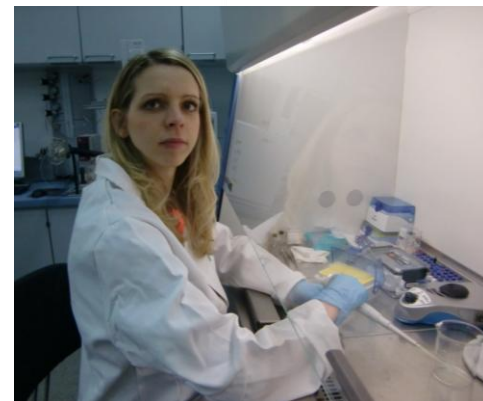
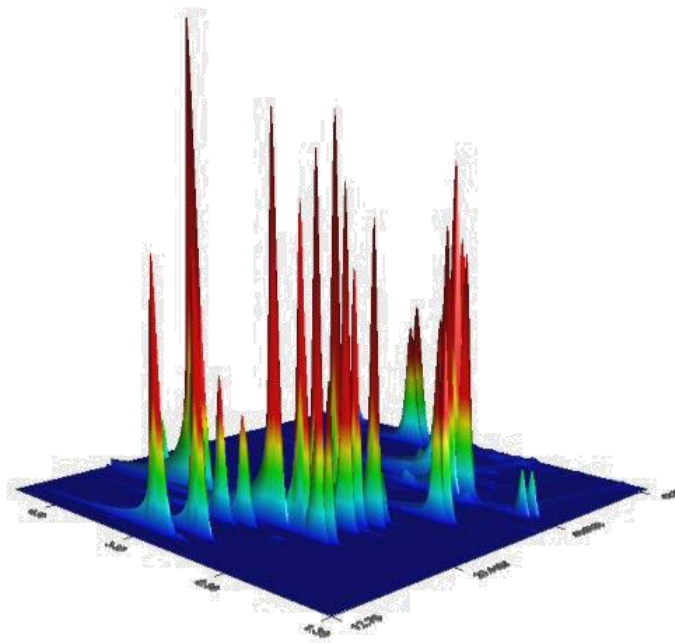
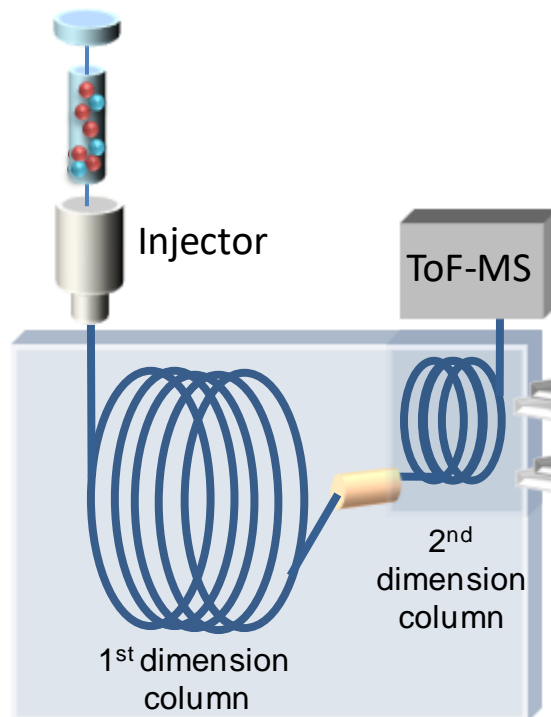


Fig. 5b: working under clean conditions...



In GC \times GC two columns are connected sequentially, typically the first dimension is a classical GC column and the second dimension is a short fast GC type, with a modulator positioned between them.

ENANTIOMER-ENRICHED AMINO ACIDS IN MURCHISON

Table 1 | Enantiomeric excesses ee_L in the Murchison meteorite.

Amino acid	ee_L (%) $\pm 3\sigma$	R_s
Proteinogenic amino acids		
Alanine	3.16 ± 0.80	4.00
Aspartic acid	4.31 ± 0.59	2.25
Valine	4.88 ± 0.73	3.20
Glutamic acid	3.79 ± 1.07	3.67
Isoleucine	9.49 ± 1.16	9.00
Leucine	26.33 ± 0.76	4.75
non-proteinogenic amino acids		
2-Aminobutyric acid	2.04 ± 0.86	3.80
3-Aminobutyric acid	5.95 ± 0.62	1.43
Norvaline	0.55 ± 0.21	4.50
Pyroglutamic acid	3.85 ± 0.78	3.20
non-proteinogenic α-dialkyl amino acids		
Isovaline	4.61 ± 0.83	1.67
Methylpyroglutamic acid	0.61 ± 0.03	3.60
Methylleucine	6.16 ± 0.26	2.00

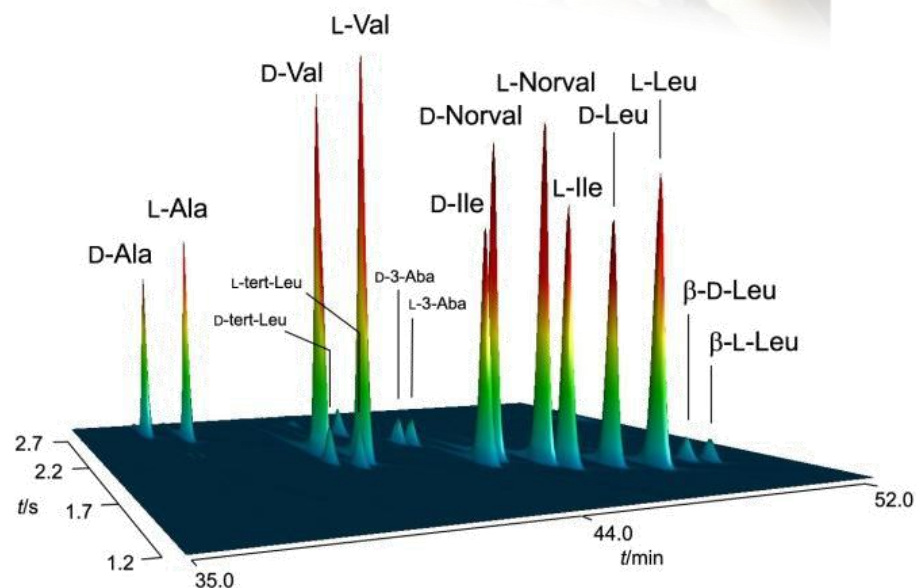


Fig. 7: Resolution of amino acid enantiomers in a sample of Murchison using ultra-modern GC \times GC coupled to TOFMS.

ENANTIOMER-ENRICHED AMINO ACIDS IN MURCHISON

Table 1 | Enantiomeric excesses ee_L in the Murchison meteorite.

Amino acid	ee_L (%) $\pm 3\sigma$	R_s
<i>Proteinogenic amino acids</i>		
Alanine	3.16 ± 0.80	4.00
Aspartic acid	4.31 ± 0.59	2.25
Valine	4.88 ± 0.73	3.20
Glutamic acid	3.79 ± 1.07	3.67
Isoleucine	9.49 ± 1.16	9.00
Leucine	26.33 ± 0.76	4.75
<i>non-proteinogenic amino acids</i>		
2-Aminobutyric acid	2.04 ± 0.86	3.80
3-Aminobutyric acid	5.95 ± 0.62	1.43
Norvaline	0.55 ± 0.21	4.50
Pyroglutamic acid	3.85 ± 0.78	3.20
<i>non-proteinogenic α-dialkyl amino acids</i>		
Isovaline	4.61 ± 0.83	1.67
Methylpyroglutamic acid	0.61 ± 0.03	3.60
Methylleucine	6.16 ± 0.26	2.00

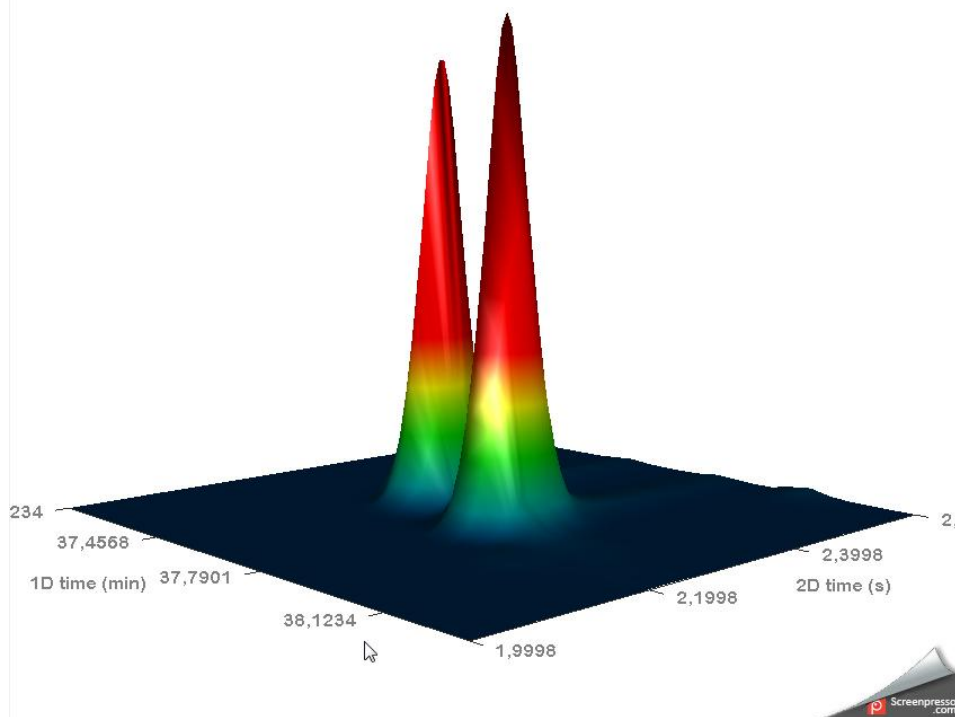


Fig. 8: Enantiomeric excess of *L*-isovaline detected in a sample of Murchison using GC \times GC-TOFMS.

Interstellar dust particle (IDP) in diffuse and dense interstellar medium

Fig. 9a: IDP with thin ice layer containing molecules such as H_2O , CO_2 , CO , CH_3OH , and NH_3 .

Fig. 9b: IDP with thick ice layer from the dense IM; in the diffuse medium this ice layer becomes irradiated by energetic UV-irradiation

Fig. 9c: In the ice mantle of the IDP photoreactions occur that form radicals and organic molecules.

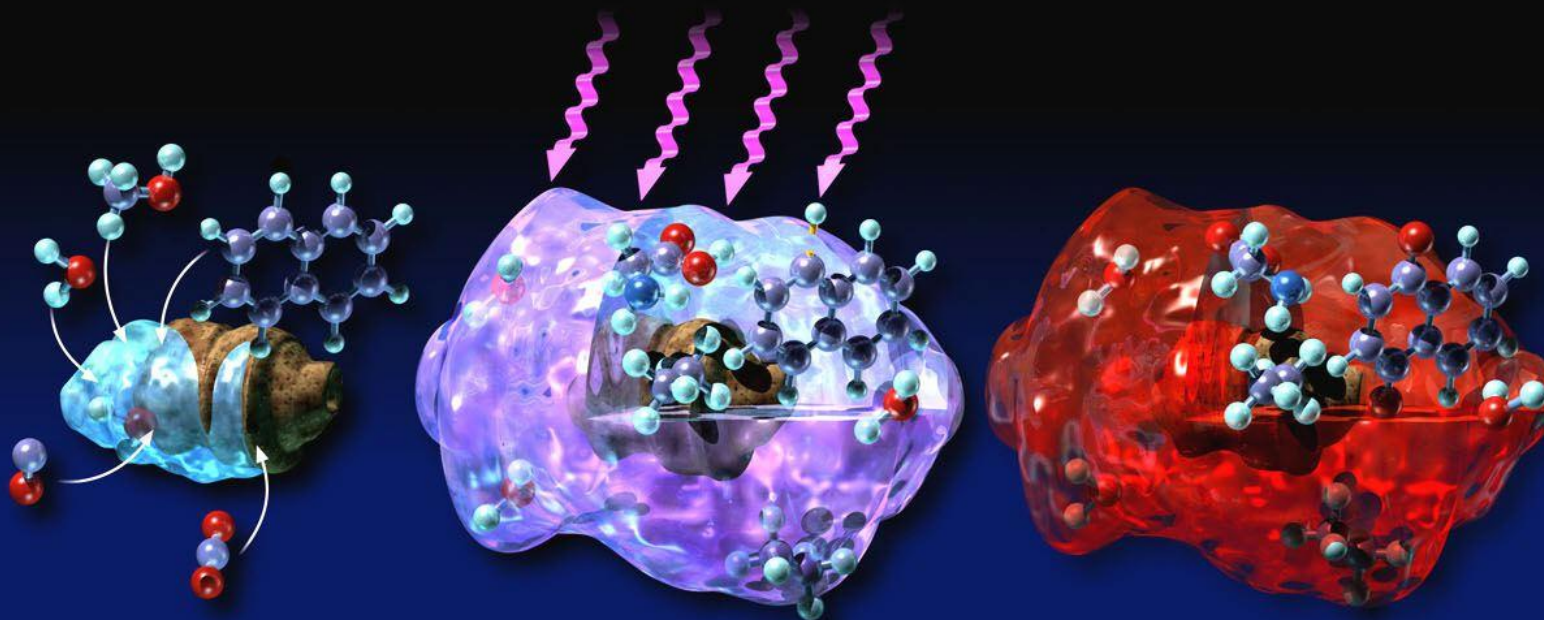
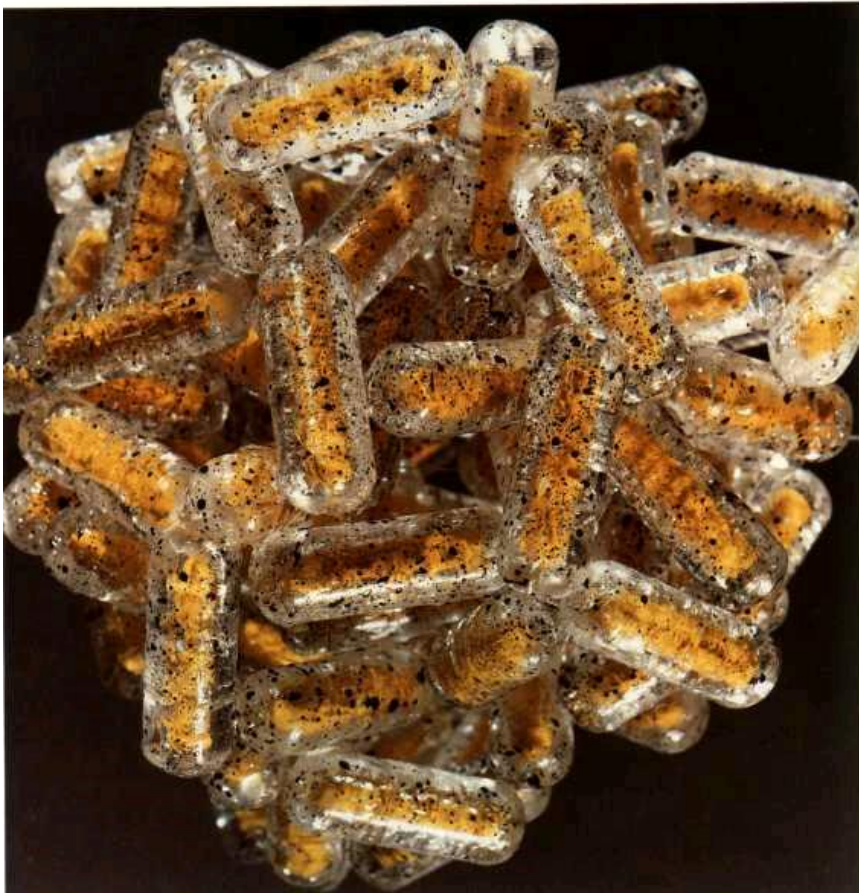


Image courtesy of Andy Christie, Slimfilms.com, Scientific American.



*Image courtesy of the Leiden
Observatory, The Netherlands*

Fig. 10: A model of a piece of a comet. Refractory yellow material is formed when condensed gases (water, carbon monoxide, carbon dioxide, methanol, ammonia) are irradiated by energetic UV light.

J. M. Greenberg *Nature* **321** (1986), 385

PRIMITIVE CHEMICAL SYNTHESIS: WHAT IS POSSIBLE UNDER SIMULATED INTERSTELLAR CONDITIONS?

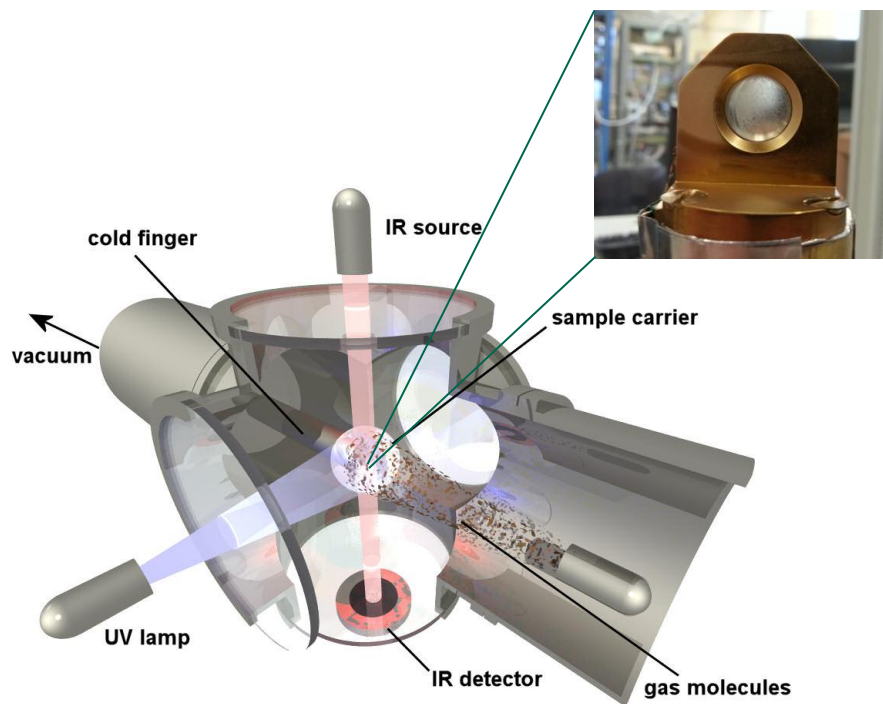


Fig. 11: Principle of a simulation chamber for interstellar photochemistry: the ice sample composed of H_2O , NH_3 , and $^{13}\text{CH}_3\text{OH}$ is deposited in the center on a MgF_2 -window at a temperature of 80 K and irradiated by vacuum UV light.

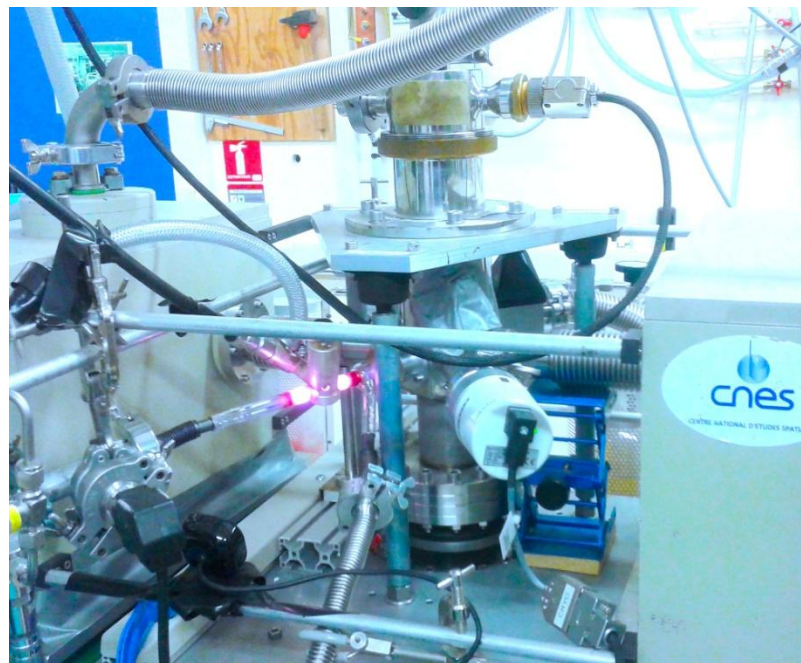
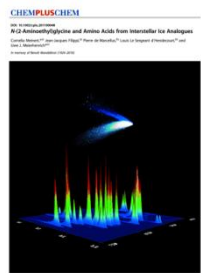


Fig 12 Space simulation chamber at the Institut d'Astrophysique Spatiale (IAS), CNRS Université Paris-Sud, Orsay.



Meinert et al. *ChemPlusChem* **77** (2012), 186–191;
Muñoz-Caro et al. *Nature* **416** (2002), 403–406.

LIFE'S BUILDING BLOCKS FORMED IN SPACE SIMULATOR . . .

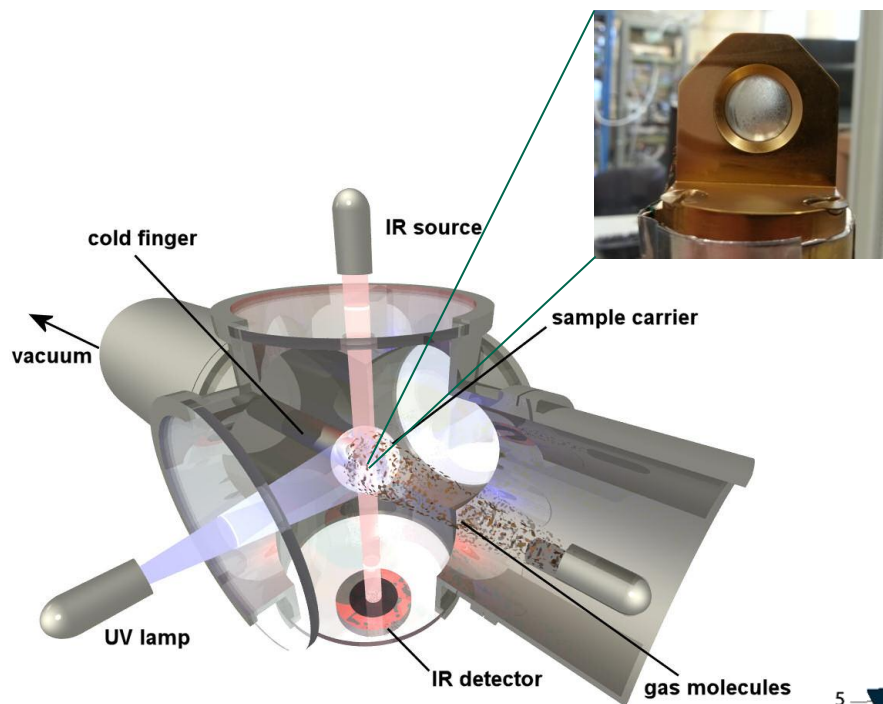


Fig. 11: Principle of a simulation chamber for interstellar photochemistry: the ice sample composed of H_2O , NH_3 , and $^{13}\text{CH}_3\text{OH}$ is deposited in the center on a MgF_2 -window at a temperature of 80 K and irradiated by vacuum UV light.

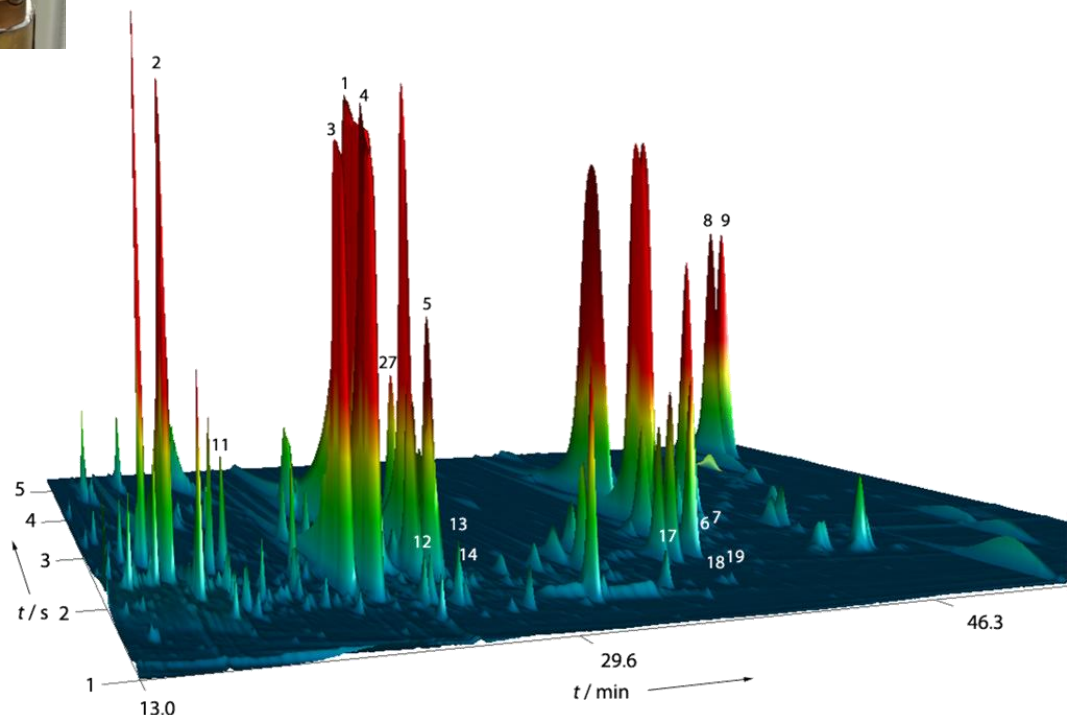
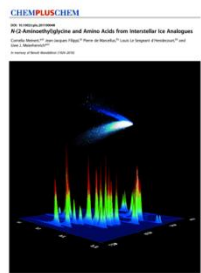


Fig. 13 GCxGC chromatogram depicting ECHFBE derivatives of ^{13}C -labelled amino acids.



Meinert et al. *ChemPlusChem* **77** (2012), 186–191;
Muñoz-Caro et al. *Nature* **416** (2002), 403–406.

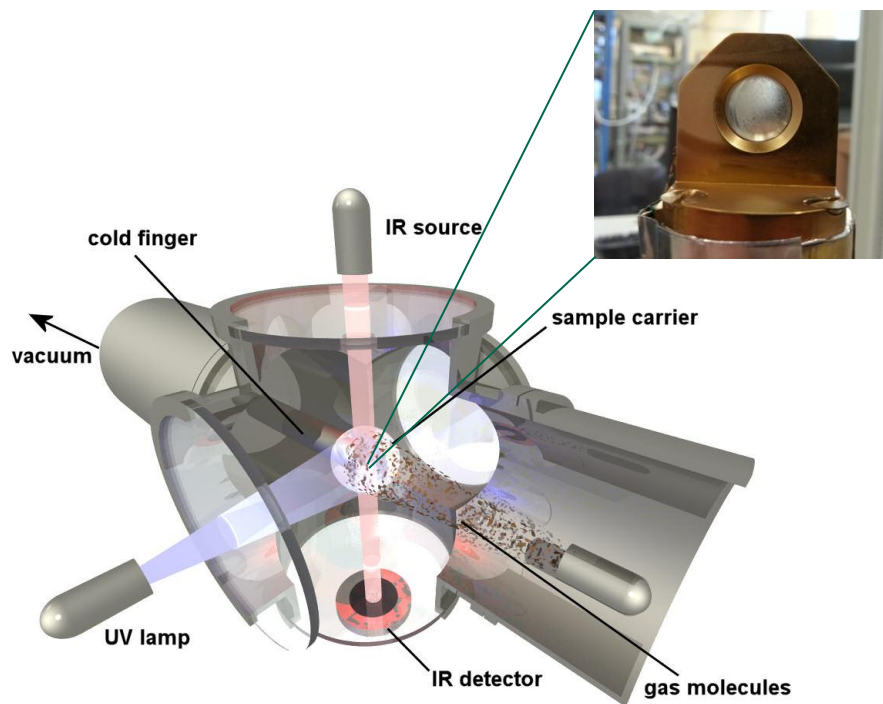
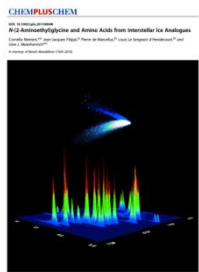


Fig. 11: Principle of a simulation chamber for interstellar photochemistry: the ice sample composed of H_2O , NH_3 , and $^{13}\text{CH}_3\text{OH}$ is deposited in the center on a MgF_2 -window at a temperature of 80 K and irradiated by vacuum UV light.



Peptide nucleic acid (PNA) based on N-(2-aminoethyl)glycine monomers

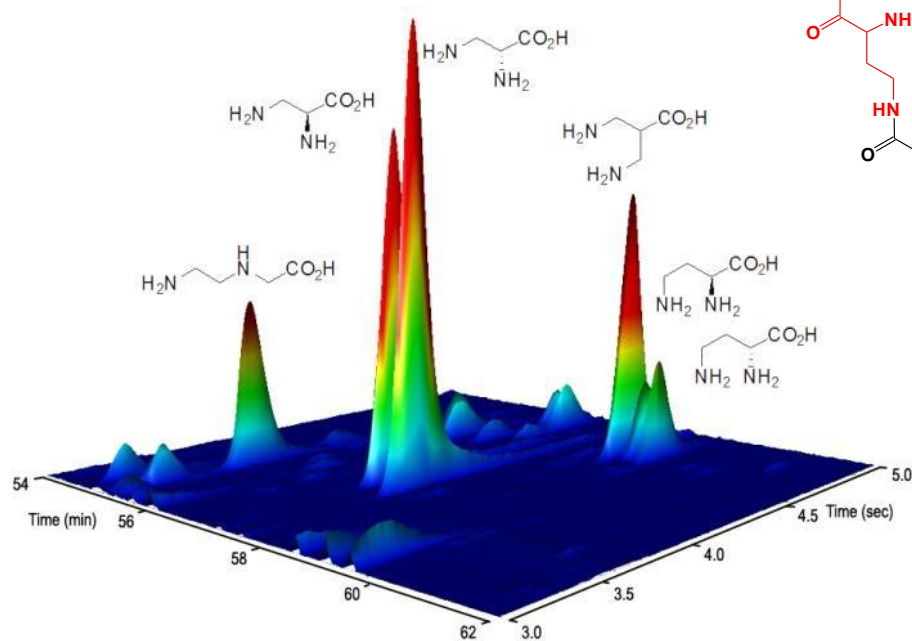
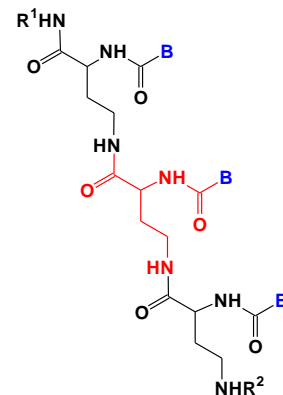


Fig. 14: Close-up view of the 2D enantioselective gas chromatogram depicting ECHFBE derivatives of ^{13}C -labelled diamino acids.

Meinert et al. *ChemPlusChem* **77** (2012), 186–191;

Muñoz-Caro et al. *Nature* **416** (2002), 403–406.

CHEMICAL EVOLUTION & THE ORIGIN OF LIFE

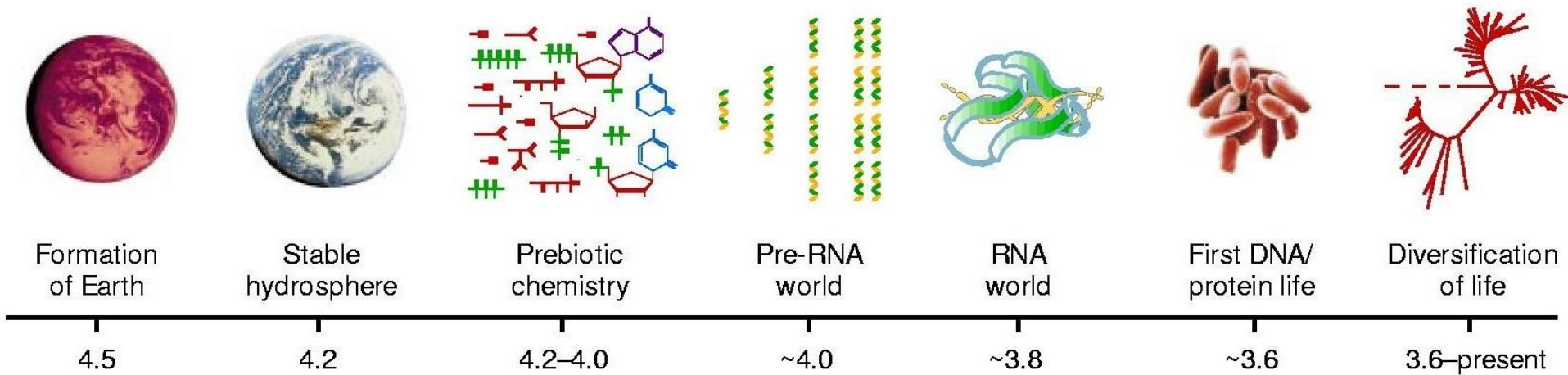


Fig.15: Timeline of events pertaining to the early history of life on Earth, with approximate dates in billions of years before the present.

Joyce G.F.: The antiquity of RNA-based evolution. *Nature* **418** (2002), 214–221

DEVELOPMENT OF GENETIC MATERIAL DURING CHEMICAL EVOLUTION

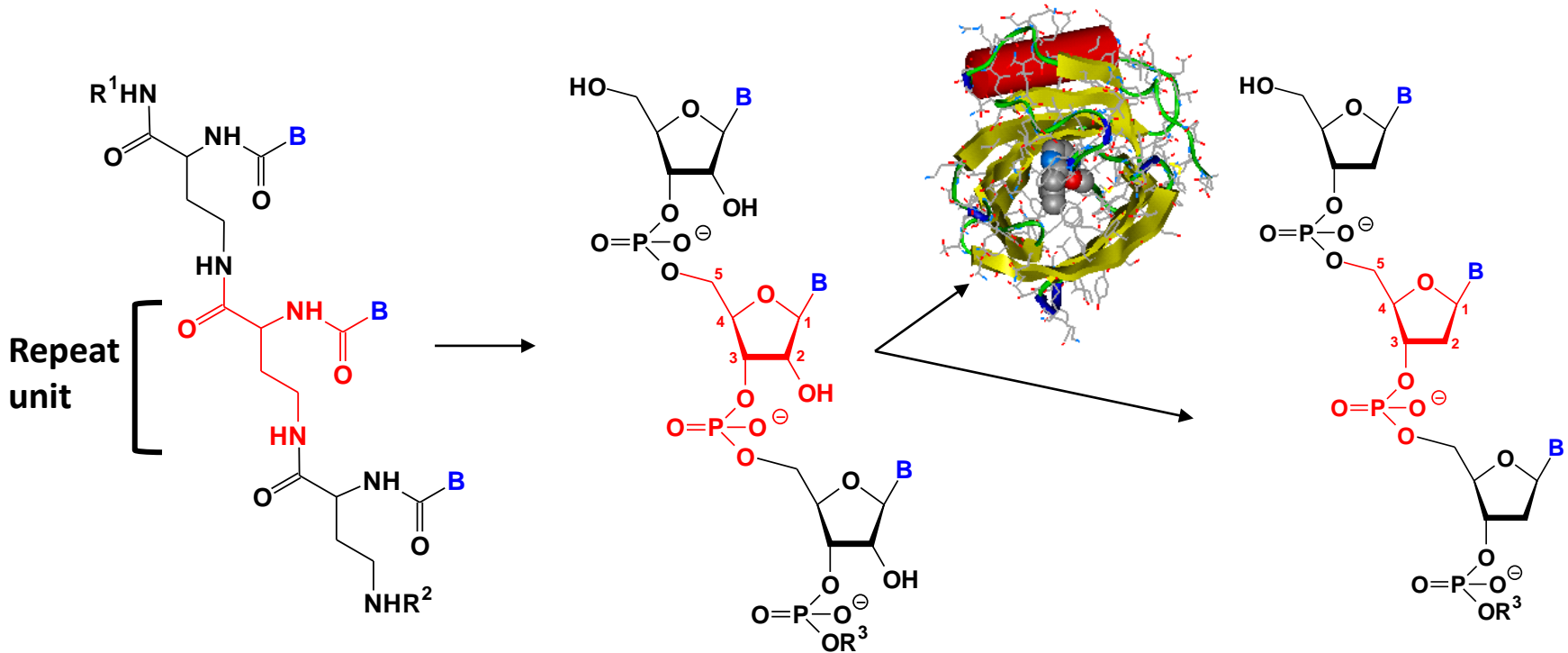


Fig. 16a: Peptide nucleic acid (PNA) based on 2,4'-diaminobutanoic acid monomers

Nielsen *et al.*: *Science* **254** (1991), 1497

Fig. 16b: Ribonucleic acid (RNA) First self-replicating molecules „RNA-World“

Gilbert: *Nature* **319** (1986), 618, D-Ribose in Furanose-Form

Fig. 16c: (TOP) Odorant binding protein including α -helix and β -sheet. **(BELOW)** Desoxyribonucleic acid (DNA). Final genetic material D-2-Desoxyribose

ALDEHYDES DETECTED IN COMETARY ANALOGUES

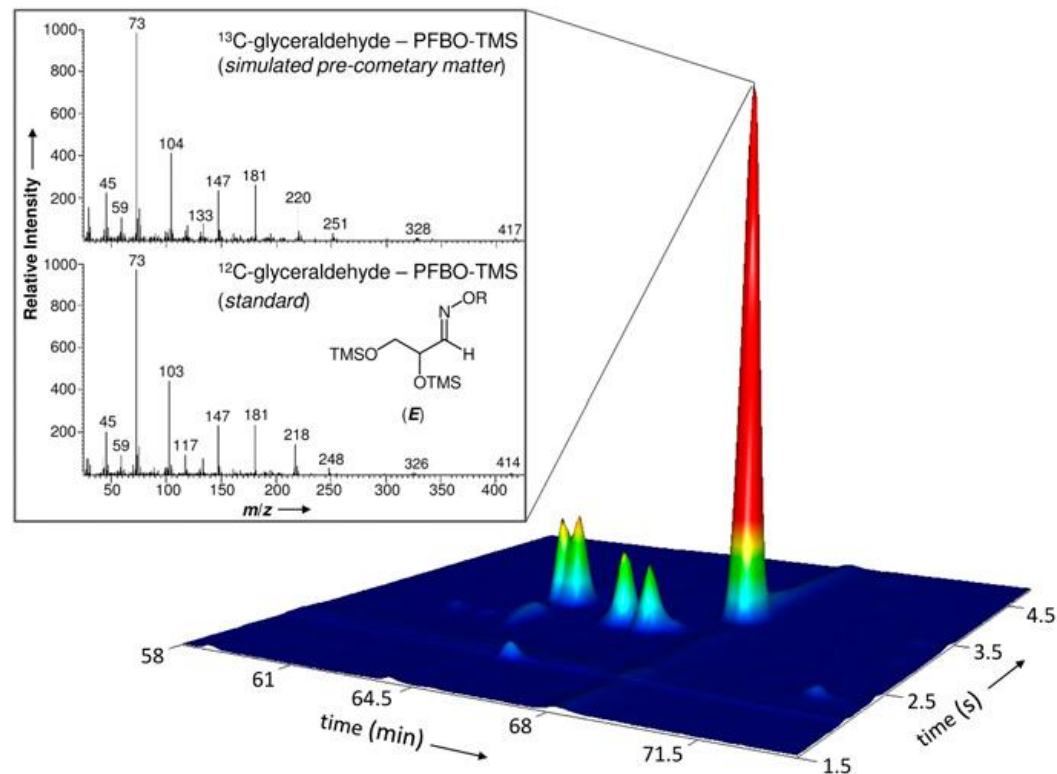
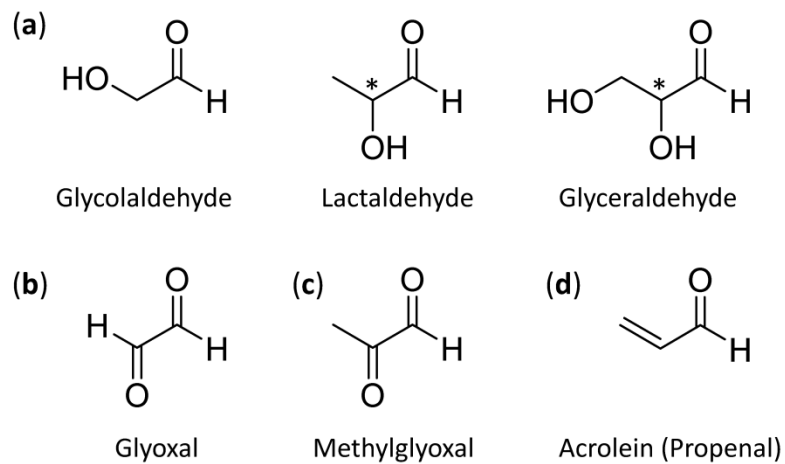


Fig. 18: Close-up view of the 2D enantioselective gas chromatogram depicting ECHFBE derivatives of ^{13}C -labelled diamino acids.

deMarcellus & Meinert et al. *PNAS* **112** (2015), 965–970.

ALTERNATIVE SYNTHESIS OF ACTIVATED RIBONUCLEOTIDES REQUIRES ALDEHYDES

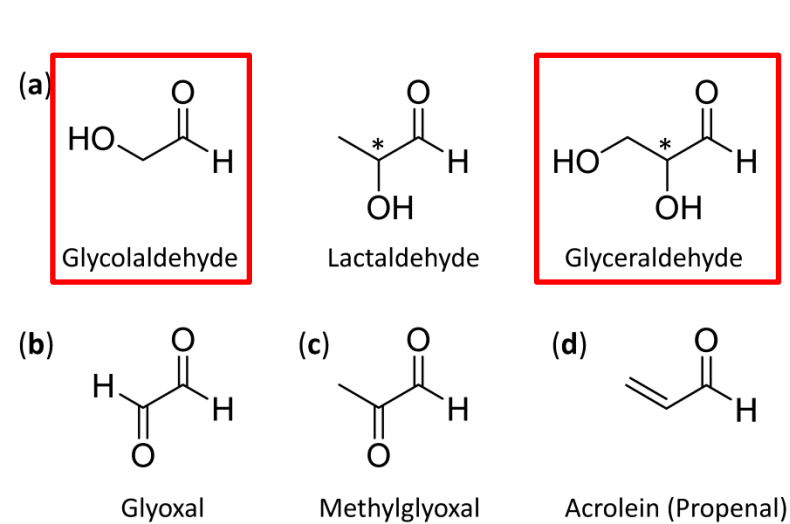
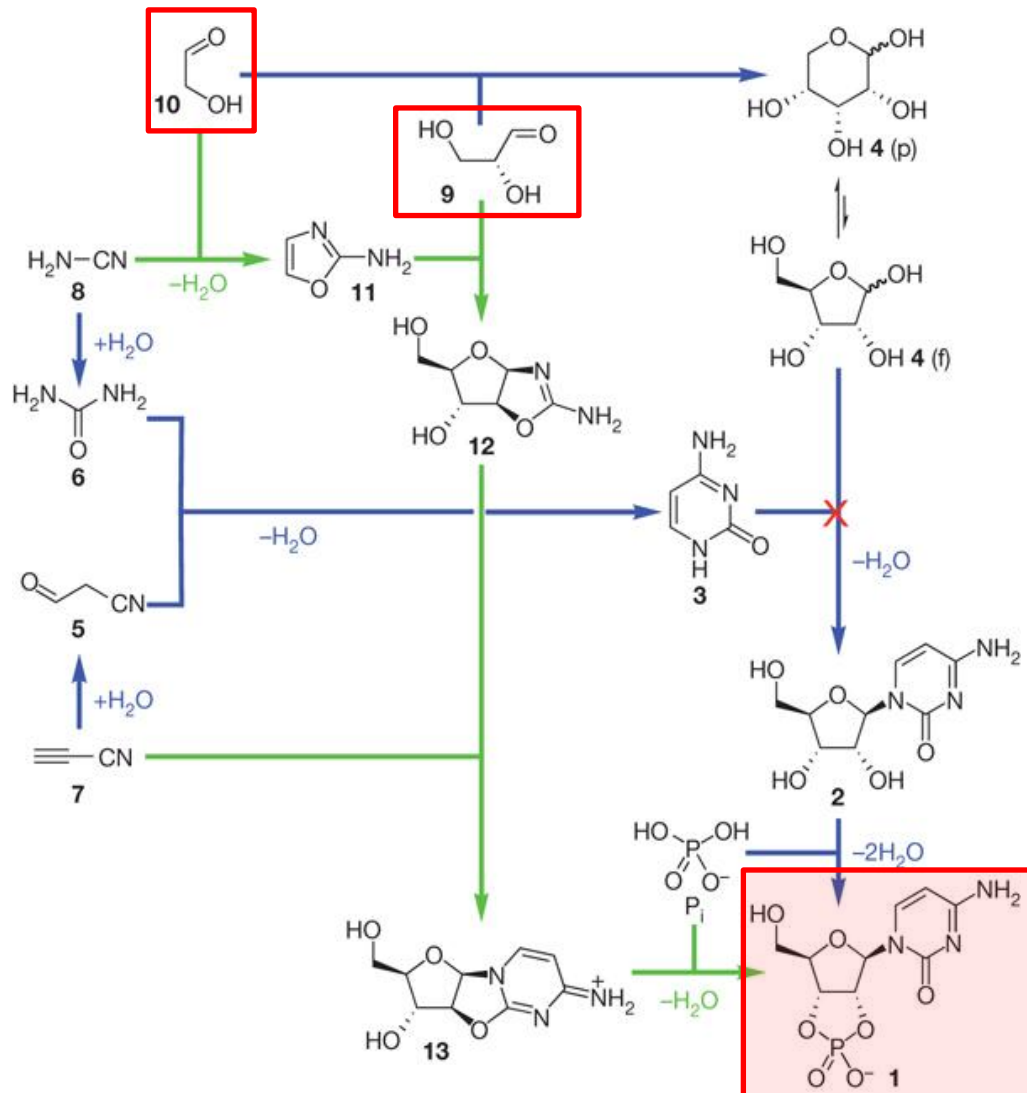


Fig. 17: Selected aldehydes identified at room temperature in simulated pre-cometary organic residues.



Sutherland et al. *Nature* **459**(2009), 239–242

RIBOSE DETECTED IN COMETARY ANALOGUES

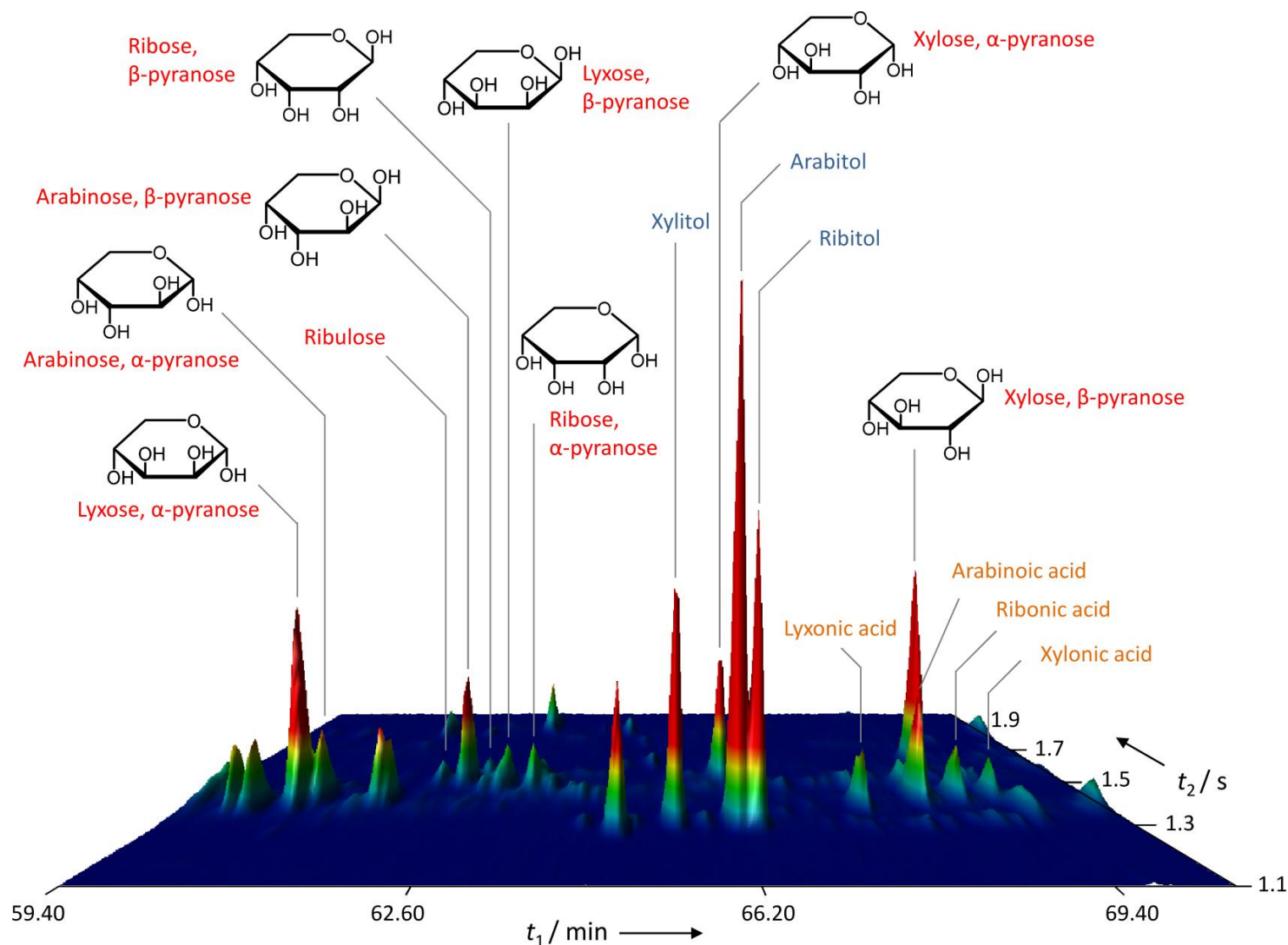


Fig. 19: RIBOSE - A key sugar found in RNA has been created in the laboratory under conditions similar to those around comets.

Meinert et al. *Science* **352** (2016), 208–212.

RIBOSE & ITS SISTER ALDOPENTOSE DETECTED IN COMETARY ANALOGUES

	Aldoses				Ketoses	
C-2	$\begin{array}{c} \text{R} \\ \\ \text{CH}_2\text{OH} \end{array}$ <p>R = CH₂OH, Ethylene glycol (550 ppm) = CHO, Glycolaldehyde (2390 ppm) = COOH, Glycolic acid (6330 ppm)</p>					
C-3	$\begin{array}{c} \text{R} \\ \\ \text{H}-\text{C}-\text{OH} \\ \\ \text{CH}_2\text{OH} \end{array}$ <p>R = CH₂OH, Glycerol (2860 ppm) = CHO, Glyceraldehyde (302 ppm) = COOH, Glyceric acid (2440 ppm)</p>				$\begin{array}{c} \text{CH}_2\text{OH} \\ \\ \text{C}=\text{O} \\ \\ \text{CH}_2\text{OH} \end{array}$ <p>Dihydroxyacetone (540 ppm)</p>	
C-4	$\begin{array}{c} \text{R} \\ \\ \text{H}-\text{C}-\text{OH} \\ \\ \text{H}-\text{C}-\text{OH} \\ \\ \text{CH}_2\text{OH} \end{array}$ <p>R = CH₂OH, Erythritol (5070 ppm) = CHO, Erythrose (< q.l.) = COOH, Erythronic acid (960 ppm)</p>		$\begin{array}{c} \text{R} \\ \\ \text{HO}-\text{C}-\text{H} \\ \\ \text{H}-\text{C}-\text{OH} \\ \\ \text{CH}_2\text{OH} \end{array}$ <p>R = CH₂OH, Threitol (7200 ppm) = CHO, Threose (< d.l.) = COOH, Threonic acid (840 ppm)</p>		$\begin{array}{c} \text{CH}_2\text{OH} \\ \\ \text{C}=\text{O} \\ \\ \text{H}-\text{C}-\text{OH} \\ \\ \text{CH}_2\text{OH} \end{array}$ <p>Erythrulose (37 ppm)</p>	
C-5	$\begin{array}{c} \text{R} \\ \\ \text{H}-\text{C}-\text{OH} \\ \\ \text{H}-\text{C}-\text{OH} \\ \\ \text{H}-\text{C}-\text{OH} \\ \\ \text{CH}_2\text{OH} \end{array}$ <p>R = CH₂OH, Ribitol (560 ppm) = CHO, Ribose (260 ppm) = COOH, Ribonic acid (82 ppm)</p>	$\begin{array}{c} \text{R} \\ \\ \text{HO}-\text{C}-\text{H} \\ \\ \text{H}-\text{C}-\text{OH} \\ \\ \text{H}-\text{C}-\text{OH} \\ \\ \text{CH}_2\text{OH} \end{array}$ <p>Arabitol (1150 ppm) Arabinose (200 ppm) Arabinoic acid (165 ppm)</p>	$\begin{array}{c} \text{R} \\ \\ \text{H}-\text{C}-\text{OH} \\ \\ \text{HO}-\text{C}-\text{H} \\ \\ \text{H}-\text{C}-\text{OH} \\ \\ \text{CH}_2\text{OH} \end{array}$ <p>Xylitol (630 ppm) Xylose (240 ppm) Xylonic acid (67 ppm)</p>	$\begin{array}{c} \text{R} \\ \\ \text{HO}-\text{C}-\text{H} \\ \\ \text{HO}-\text{C}-\text{H} \\ \\ \text{H}-\text{C}-\text{OH} \\ \\ \text{CH}_2\text{OH} \end{array}$ <p>Arabitol (1150 ppm) Lyxose (145 ppm) Lyxonic acid (140 ppm)</p>	$\begin{array}{c} \text{CH}_2\text{OH} \\ \\ \text{C}=\text{O} \\ \\ \text{H}-\text{C}-\text{OH} \\ \\ \text{H}-\text{C}-\text{OH} \\ \\ \text{CH}_2\text{OH} \end{array}$ <p>Ribulose (2010 ppm)</p>	$\begin{array}{c} \text{CH}_2\text{OH} \\ \\ \text{C}=\text{O} \\ \\ \text{HO}-\text{C}-\text{H} \\ \\ \text{H}-\text{C}-\text{OH} \\ \\ \text{CH}_2\text{OH} \end{array}$ <p>Xylulose (470 ppm)</p>

RIBOSE & ITS SISTER ALDOPENTOSEs FORMED *via* « INTERSTELLAR FORMOSE REACTION »

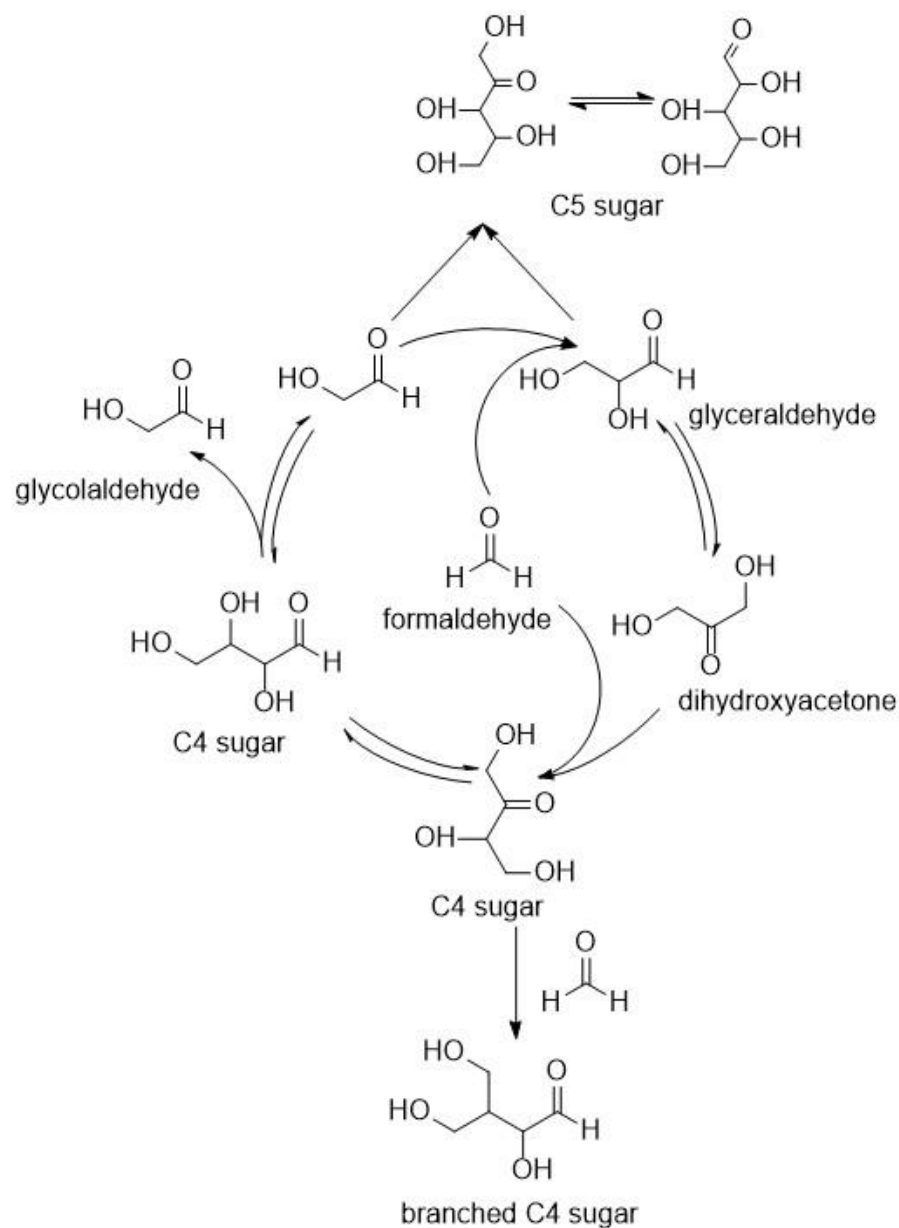
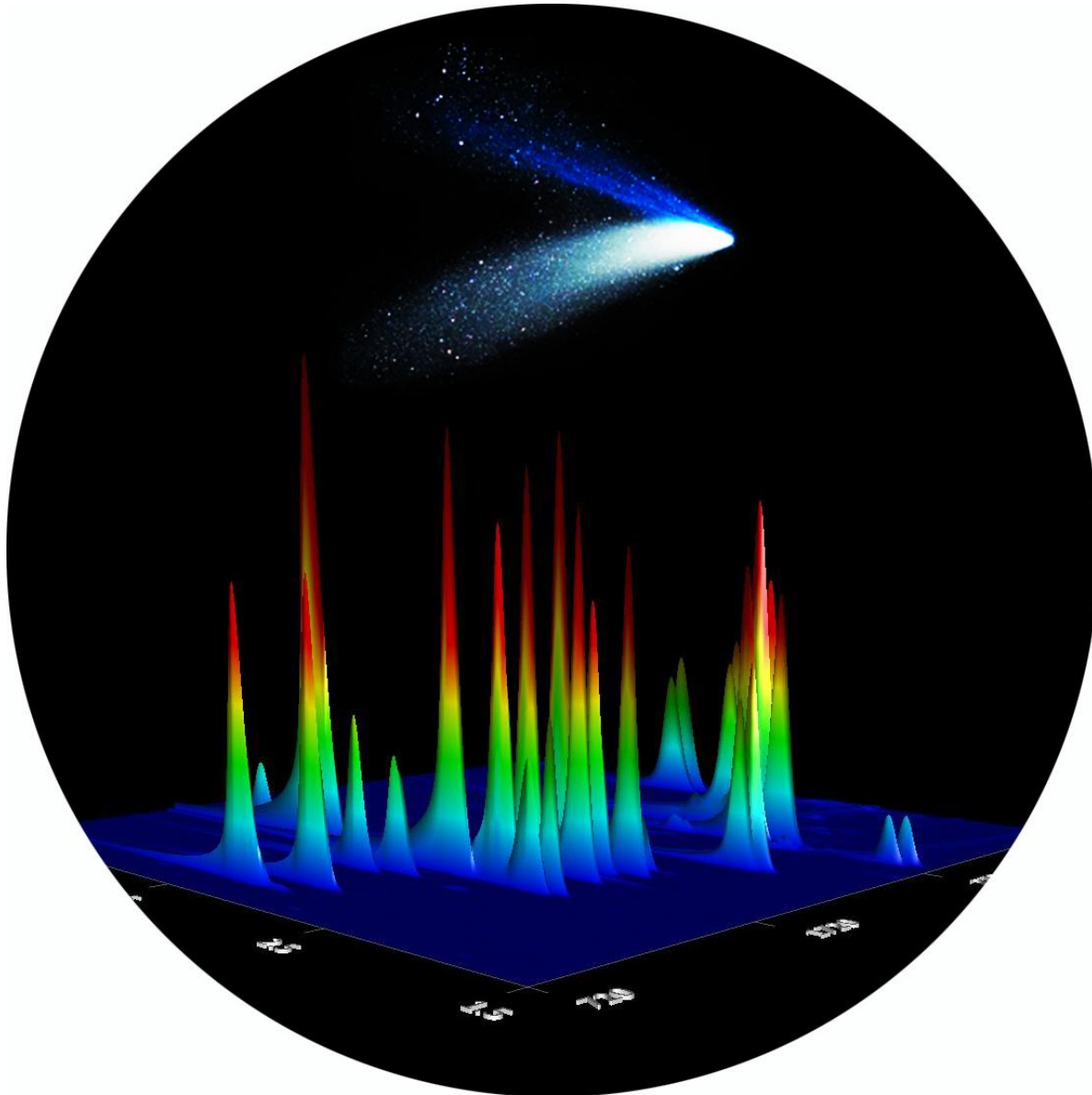


Fig. 20: The formose reaction. Formaldehyde condenses under autocatalytic reaction kinetics to form **glycolaldehyde**, which undergoes an aldol reaction by forming **glyceraldehyde**. C3 sugar molecules react with **Glycolaldehyde** forming pentulose, which isomerizes to an aldopentose such as **ribose**.

AMINO ACIDS & SUGAR COMPOUNDS IN COMETARY MATTER ?



ROSETTA –

INTERNATIONAL MISSION TO A COMET, IN SEARCH OF LIFE'S ORIGIN

An activist uses science to
fight animal research p. 368 | A battle of principles in the
e-cigarettes debate p. 373 | Counting molecular garbage
clutes in intact neurons p. 419

Science

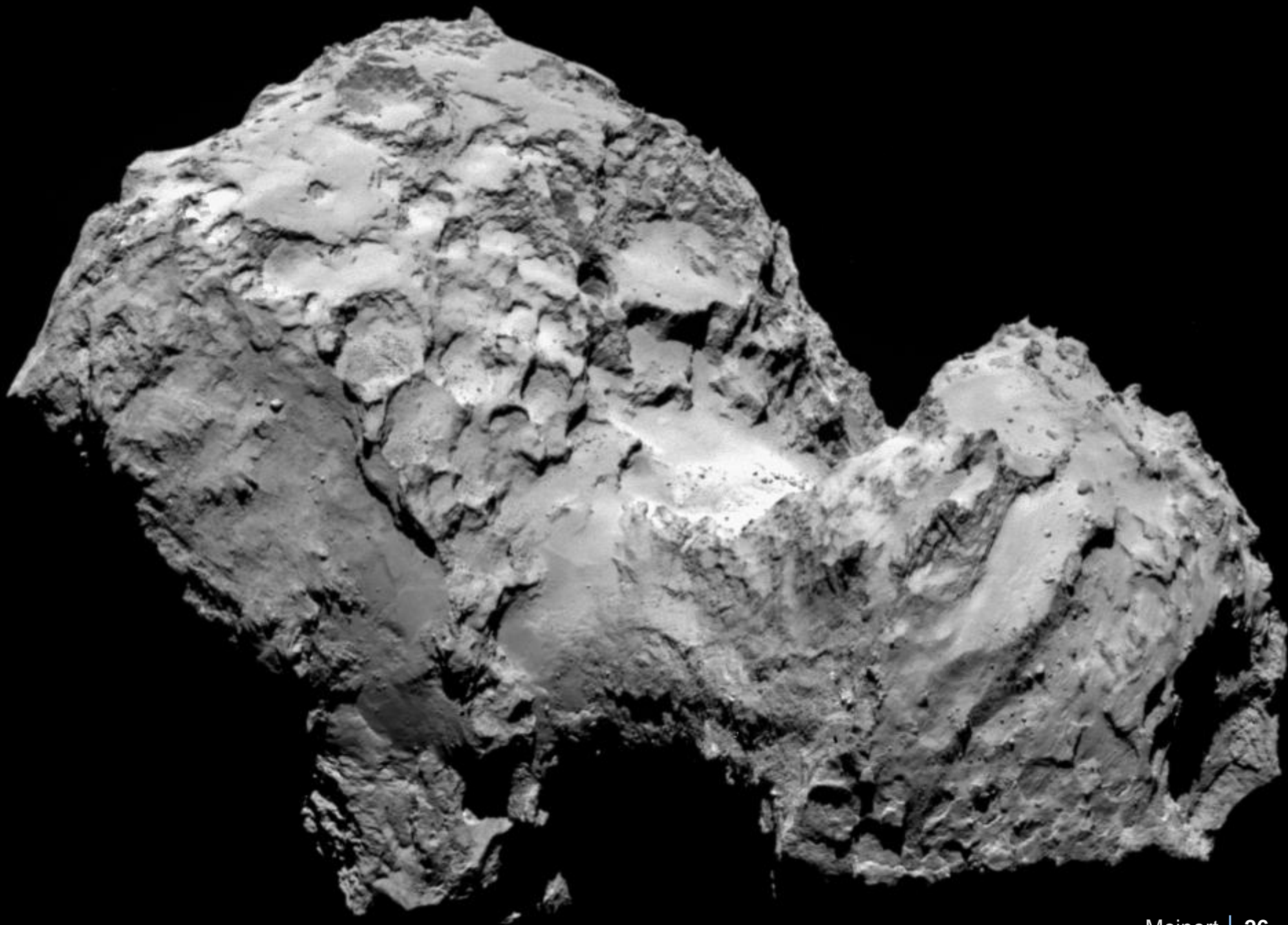
\$10
23 JANUARY 2015
science.org

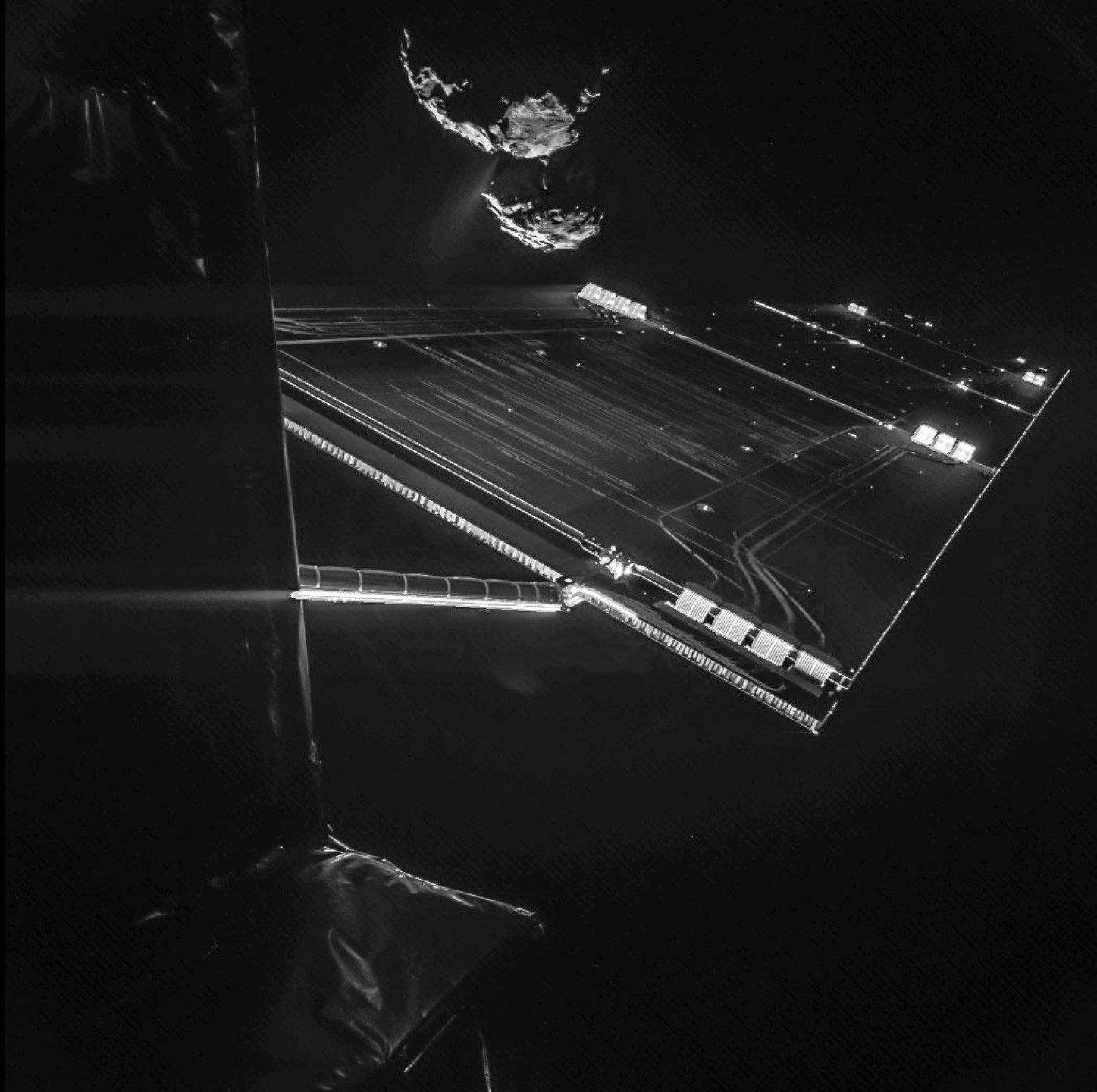
AAAS

Catching a comet

Rosetta follows a relic
of the early solar system
toward the Sun
pp. 358 & 387







RESEARCH ARTICLE

SPACE SCIENCES

Prebiotic chemicals—amino acid and phosphorus—in the coma of comet 67P/Churyumov-Gerasimenko

Kathrin Altwegg,^{1,2*} Hans Balsiger,¹ Akiva Bar-Nun,³ Jean-Jacques Berthelier,⁴ Andre Bieler,^{1,5} Peter Bochsler,¹ Christelle Briois,⁶ Ursina Calmonte,¹ Michael R. Combi,⁵ Hervé Cottin,⁷ Johan De Keyser,⁸ Frederik Dhooghe,⁸ Bjorn Fiethe,⁹ Stephen A. Fuselier,¹⁰ Sébastien Gasc,¹ Tamas I. Gombosi,⁵ Kenneth C. Hansen,⁵ Myrtha Haessig,^{1,10} Annette Jäckel,¹ Ernest Kopp,¹ Axel Korth,¹¹ Lena Le Roy,² Urs Mall,¹¹ Bernard Marty,¹² Olivier Mousis,¹³ Tobias Owen,¹⁴ Henri Rème,^{15,16} Martin Rubin,¹ Thierry Sémon,¹ Chia-Yu Tzou,¹ James Hunter Waite,¹⁰ Peter Wurz¹

2016 © The Authors, some rights reserved;
exclusive licensee American Association for
the Advancement of Science. Distributed
under a Creative Commons Attribution
NonCommercial License 4.0 (CC BY-NC).
10.1126/sciadv.1600285

The importance of comets for the origin of life on Earth has been advocated for many decades. Amino acids are key ingredients in chemistry, leading to life as we know it. Many primitive meteorites contain amino acids, and it is generally believed that these are formed by aqueous alterations. In the collector aerogel and foil samples of the Stardust mission after the flyby at comet Wild 2, the simplest form of amino acids, glycine, has been found together with precursor molecules methylamine and ethylamine. Because of contamination issues of the samples, a cometary origin was deduced from the ¹³C isotopic signature. We report the presence of volatile glycine accompanied by methylamine and ethylamine in the coma of 67P/Churyumov-Gerasimenko measured by the ROSINA (Rosetta Orbiter Spectrometer for Ion and Neutral Analysis) mass spectrometer, confirming the Stardust results. Together with the detection of phosphorus and a multitude of organic molecules, this result demonstrates that comets could have played a crucial role in the emergence of life on Earth.

INTRODUCTION

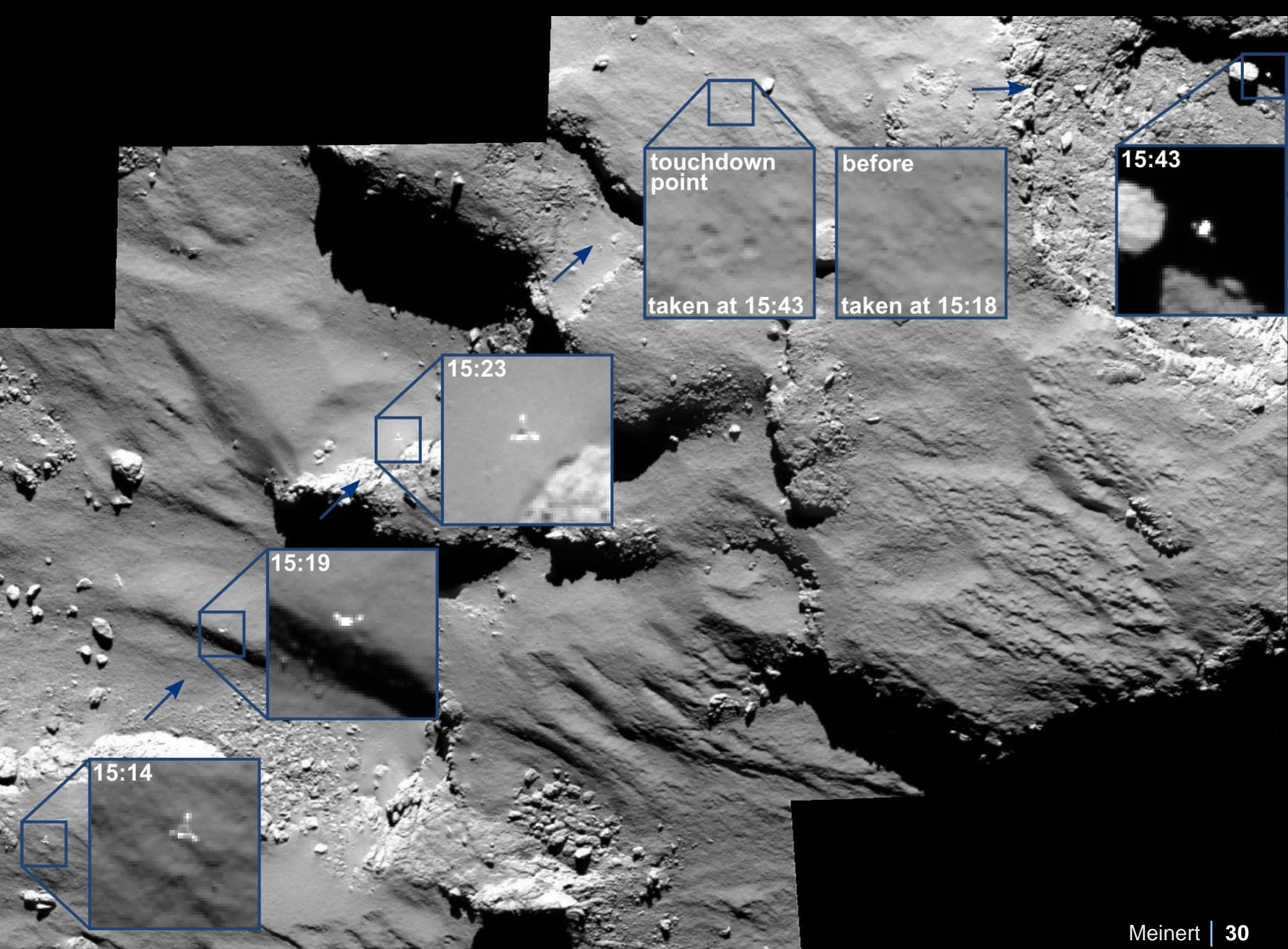
The possibilities that organic molecules were brought to the early Earth through impacts of small bodies and that these molecules contributed to spark the emergence of life have been the subject of significant debates (1). Many primitive meteorites contain amino acids (2), and it is generally believed that these are formed by aqueous alterations within the parent bodies during the early stages (3).

glycine is not among them. In contrast, methylamine has been observed in the interstellar medium (ISM) (6). There was a rigorous attempt to verify the presence of glycine in the ISM by Snyder *et al.* (7) after a tentative detection by Kuan *et al.* (8). This attempt concluded that the observed lines do not prove the existence of glycine in the ISM. The sublimation temperature of glycine is below 150°C (9).

Downloaded from <http://advances.sciencemag.org/>

12 Novembre 2014 : Atterrissage !





touchdown
point

before

15:43

taken at 15:43

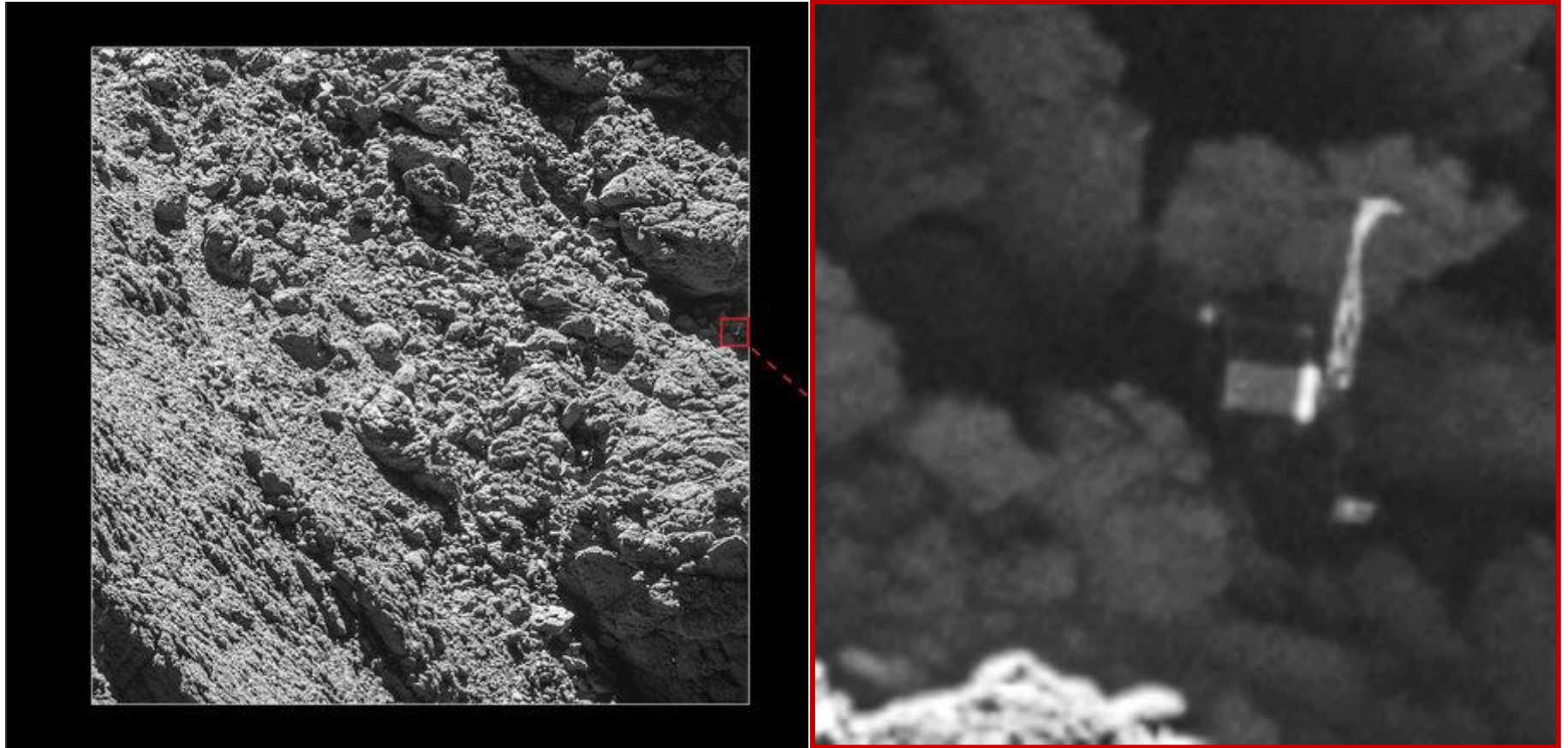
taken at 15:18

15:23

15:19

15:14

PHILAE FOUND!



The images were taken **on 2 September 2016** by the OSIRIS narrow-angle camera as the orbiter came within 2.7 km of the surface and clearly show the main body of the lander, along with two of its three legs.

SCIENTIFIC INSTRUMENTS OF THE PHILAE LANDER

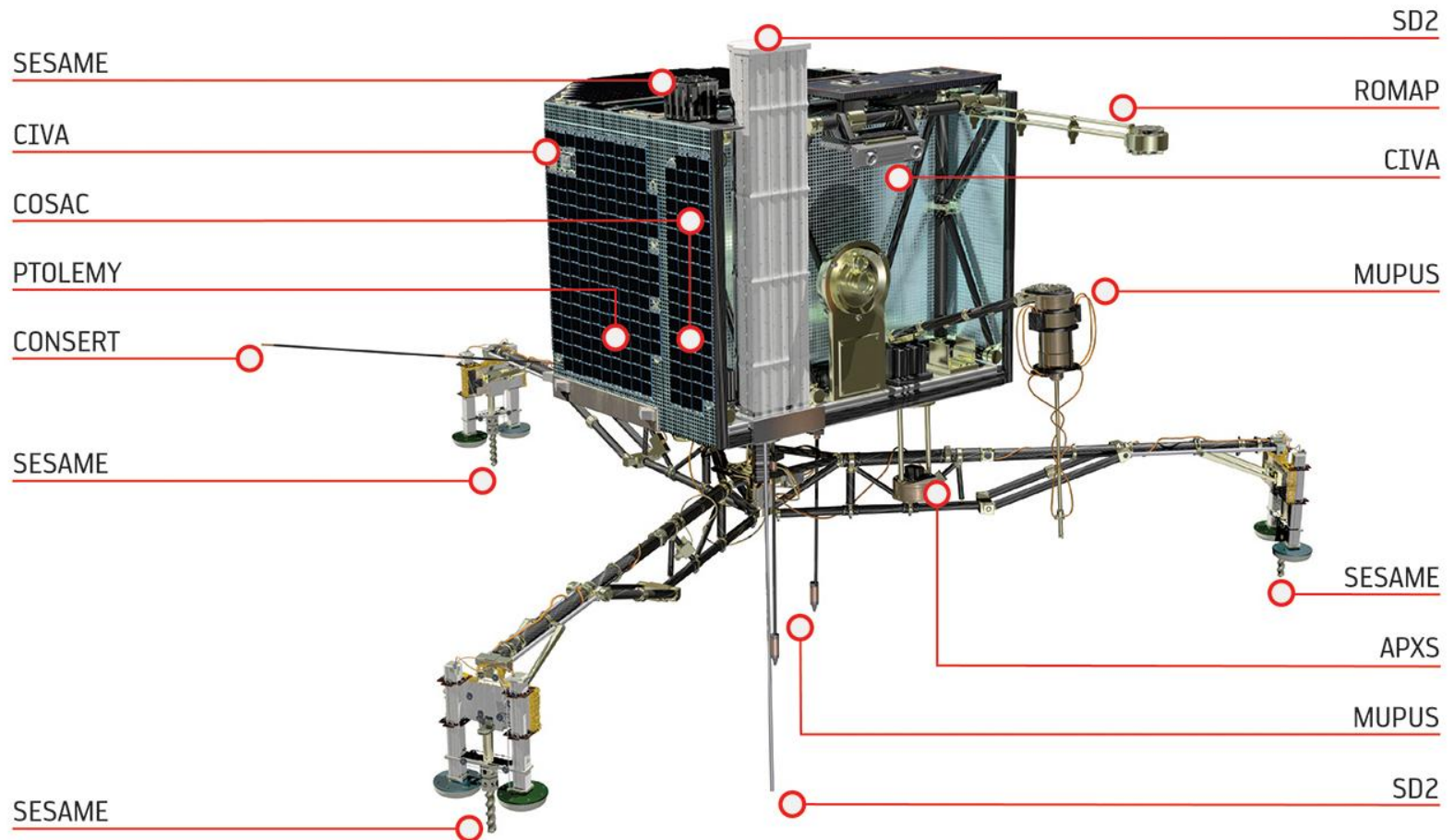


Fig. 21: Scientific instruments of the Philae lander. This view shows the 'balcony', which is an experiment carrier located in front of the hood that covers the warm compartment and carries the solar generator

GENERALIZED FORMATION SCHEME OF 67P-COMPOUNDS IDENTIFIED BY COSAC / ROSETTA

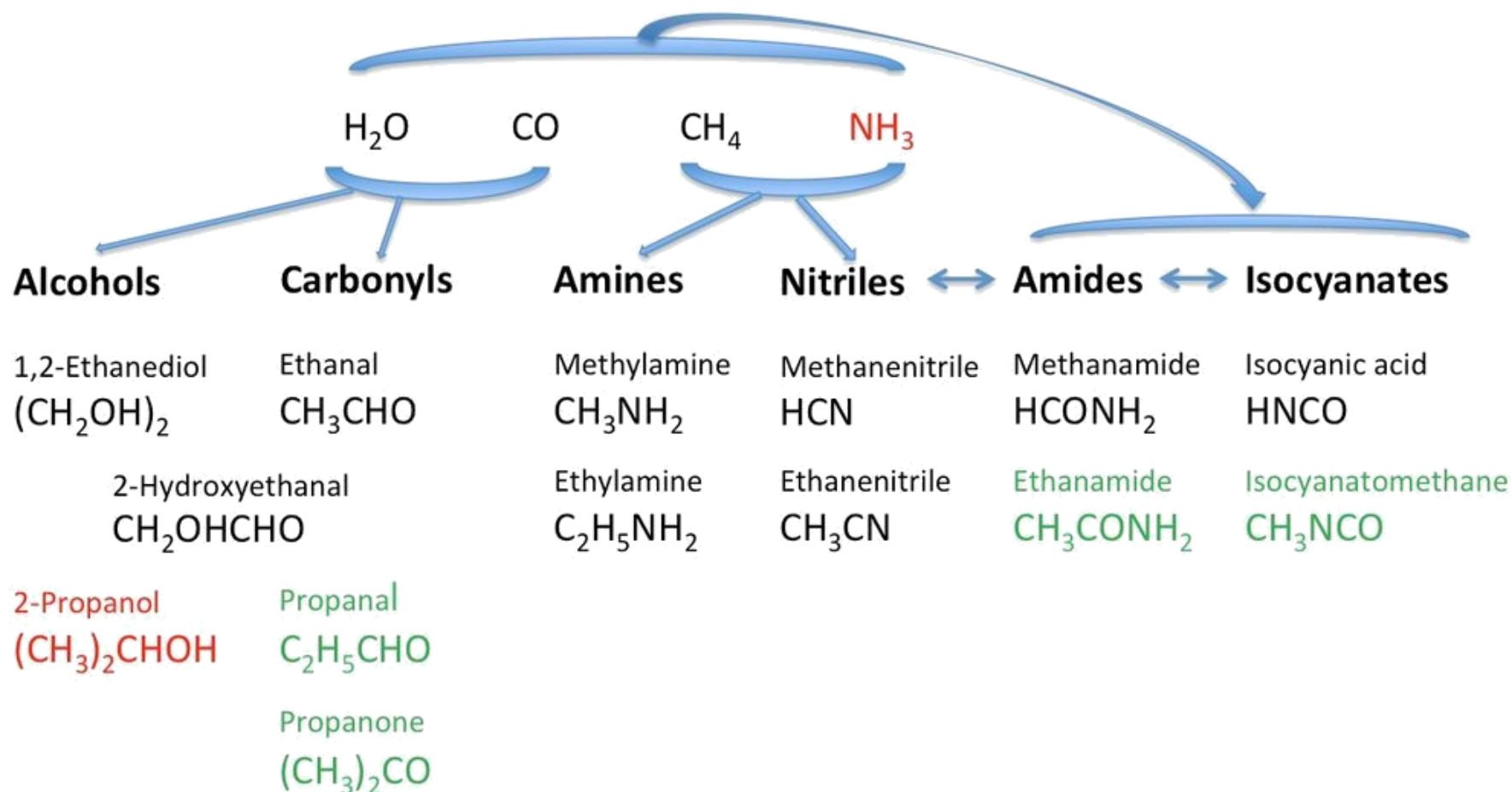


Fig. 22: Possible formation pathways of COSAC compounds. Species in red not confidently identified, species in green reported for the first time in comets by COSAC.

F. Goesmann et al., *Science* **349** (2015), aab0689.

SPACE SCIENCES

Prebiotic chemicals—amino acid and phosphorus—in the coma of comet 67P/Churyumov-Gerasimenko

Kathrin Alt
Christelle E
Bjorn Fieth
Annette Jä
Tobias Owi

The importan
key ingredie
is generally b
Stardust mis
together with
a cometary
accompanie
the ROSINA
Stardust res
demonstrate

INTRODUC

The possibi
Earth throug

Evider in the

by
KEITH KV
JAMES LA
KATHERIN
ETTA PET
JOSE FLO
CYRIL PO
Exobiology C
Ames Resear
Moffett Field
California 94

THE Opin
postulating
the appear
by experim
cules impor
conditions
planet^{6,7}. I
would be 1
pounds of
conditions.

Recent s
niques of 1
water^{8,9}, an
carbon m
considered
biochemica
for the pos
and poly
medium.

Apollo 12 missions provi

Carbonaceous meteorites as a source of sugar-related organic compounds

fo

Geo
Kat

* N
† In
Uni

The
sta
ma
in c
to
pla
(pe
all
DN

removed, and the solution added to an equal volume of 12M HCl (Ultrax II ultrapure reagent, Baker) and heated for 16 h at 100 °C in an organic-free sealed glass ampoule. This material was dried *in vacuo* to remove water, HCl and any volatile organic acids, then

923

letters to nature

has hitherto been no conclusive evidence for the existence of polyols in meteorites, leaving a gap in our understanding of the origins of biologically important organic compounds on Earth. Here we report that a variety of polyols are present in, and indigenous to, the Murchison and Murray meteorites in amounts

letters to nature

Acknowledgements

This work was supported by NASA grants from the Origins of Solar Systems, Exobiology, and Astrobiology programmes, as well as the NASA Ames Director's Discretionary Fund.

Aldehydes and sugars from evolved precometary ice analogs: Importance of ices in astrochemical and prebiotic

Pierre de Marcell
Louis Le Sergean

^aUniversité Paris-Sud,
Nice, UMR 7272, CNRS
Autónoma del Estado

Edited by Mark H. Thi

Evolved interstellar clouds may argue materials that will a wealth of experiments reproduce these ices are routine identifications in that we have searched prebiotic interest, coupled to time-of 10 aldehydes, including glyceraldehyde—t mediates in the first in a planetary environment and methanol ice

ASTROCHEMISTRY

Ribose and related sugars from ultraviolet irradiation of interstellar ice analogs

Cornelia Meinert,^{1,*} Iuliia Myrgorodska,^{1,2} Pierre de Marcellus,³ Thomas Buhse,⁴ Laurent Nahon,⁵ Søren V. Hoffmann,⁵ Louis Le Sergeant d'Hendecourt,³ Uwe J. Meierhenrich^{1,*}

Ribose is the central molecular subunit in RNA, but the prebiotic origin of ribose remains unknown. We observed the formation of substantial quantities of ribose and a diversity of structurally related sugar molecules such as arabinose, xylose, and lyxose in the room-temperature organic residues of photo-processed interstellar ice analogs initially composed of H₂O, CH₃OH, and NH₃. Our results suggest that the generation of numerous sugar molecules, including the aldopentose ribose, may be possible from photochemical and thermal treatment of cosmic ices in the late stages of the solar nebula. Our detection of ribose provides plausible insights into the chemical processes that could lead to formation of biologically relevant molecules in suitable planetary environments.

DNA is the genetic source code for all known living organisms. It is currently thought that DNA evolved from a primordial ribonucleic acid (RNA) world state (1, 2), in which ribose chemically binds and orien-

tates the complementary purine and pyrimidine nucleobases for efficient base pairing. Ribose thereby forms the essential part of the RNA backbone. However, ribose is difficult to form, and the source of the ribose subunits in the sugars that consti-

tute the key stereodictating elements in nucleic acid structure remained unknown (3, 4). We describe here the identification of precursor molecules, including ribose, in simulated precometary ices using the sensitive two-dimensional gas chromatography time-of-flight mass spectrometry (GC×GC-TOFMS) technique.

Our astrophysical scenario involves the simulation of the photo- and thermo-chemistry of precometary ices. It is based on the assumption that planetesimals (including asteroids, comets, and the parent bodies of meteorites) were formed in the solar nebula from the aggregation of icy grains

¹Université Nice Sophia Antipolis, Institut de Chimie de Nice, UMR 7272 CNRS, 28 Avenue Valrose, 06108 Nice, France.

²Synchrotron SOLEIL, L'Orme des Merisiers, St Aubin BP48, 91192 Gif-sur-Yvette, France. ³Institut d'Astrophysique Spatiale, CNRS, Université Paris-Sud, Université Paris-Saclay, bât. 121, 91405 Orsay, France. ⁴Centro de Investigaciones Químicas, Universidad Autónoma del Estado de Morelos, Avenida Universidad 1001, 62209 Cuernavaca, Mexico.

⁵Aarhus University, Department of Physics and Astronomy, Ny Munkegade 120, 8000 Aarhus, Denmark.

*Corresponding author. E-mail: cornelia.meinert@unice.fr (C.M.); uwe.meierhenrich@unice.fr (U.J.M.)

Fig. 1. Aldoses and ketoses as identified in a sample generated under simulated precometary

Aldoses	Ketoses
R CH ₂ OH	R = CH ₂ OH, Ethylene glycol (550 ppm) = CHO, Glyceraldehyde (2390 ppm)

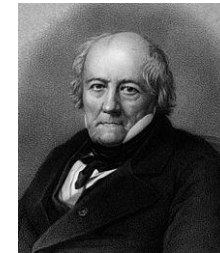
A Brief Refresher:

1. **Optical activity** was first demonstrated in 1812, when french physicist Jean Baptiste Biot discovered that **quartz crystals could rotate a beam of plane-polarized light**. He also determined that many natural products (ex. turpentine, camphor, tartaric acid) also had this property.

2. In 1848, Pasteur separated sodium ammonium **tartrate crystals into two different forms** (now known as enantiomers) and showed that they had identical properties with the exception of the rotation of polarized light.

*Since both the salt as well as dissolved solutions of the salt displayed optical activity, this demonstrated that **optical activity** was not a property of the crystals, but rather a **property of the molecules themselves**.*

3. In 1874, Jacobus Van't Hoff and Joseph Le Bel proposed the concept of the tetrahedral carbon, stereocenters, and chirality



Jean Baptiste Biot



Louis Pasteur



Joseph Le Bel



Jacobus Van't Hoff

MOLECULES CAN BE CHIRAL, SUCH AS HANDS ARE!

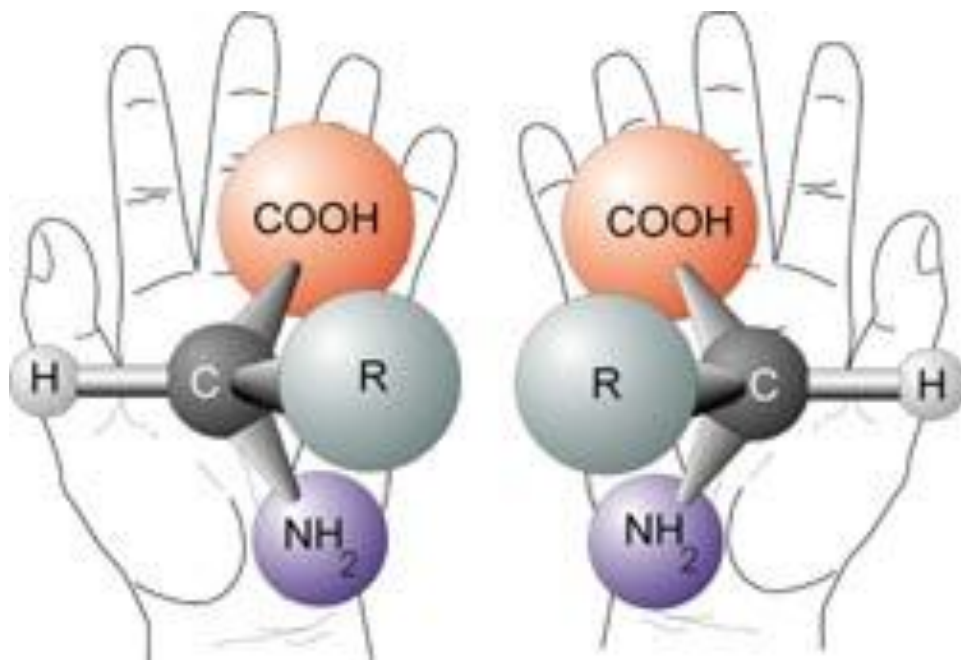


Fig. 23: Chiral compounds exist as **enantiomers** which are non-superimposable mirror images of each other.



MOLECULES CAN BE CHIRAL, SUCH AS HANDS ARE!

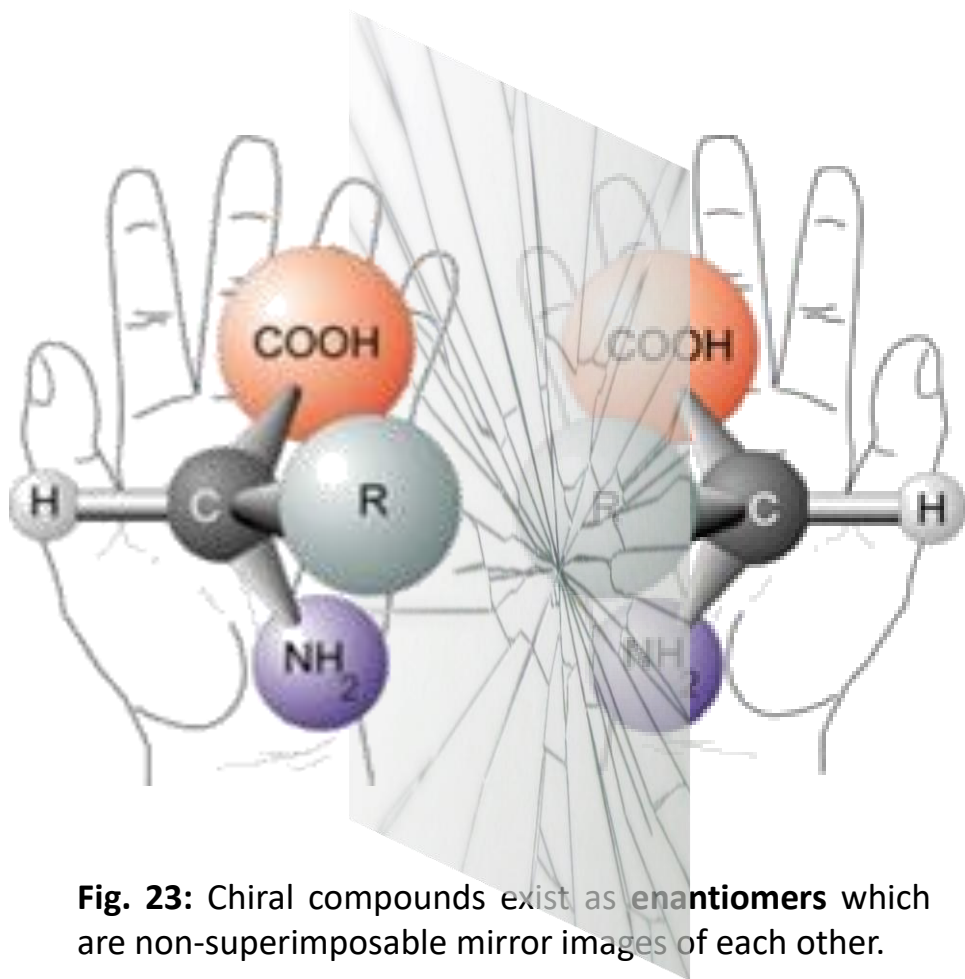
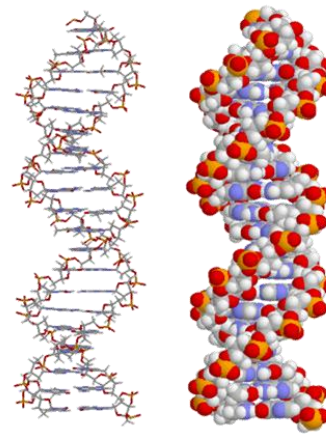
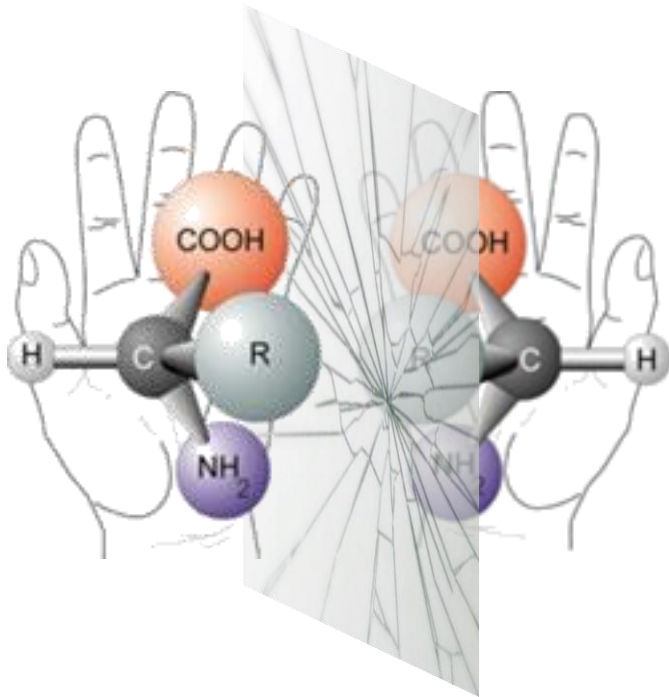


Fig. 23: Chiral compounds exist as **enantiomers** which are non-superimposable mirror images of each other.

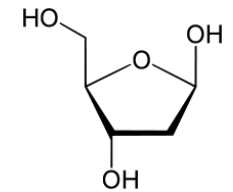


HOMOCHIRALITY OF LIFE!



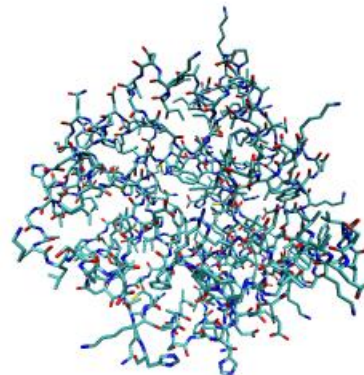
DNA

chiral
monomer



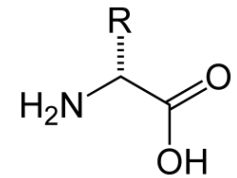
D-2-deoxyribose

carbohydrates



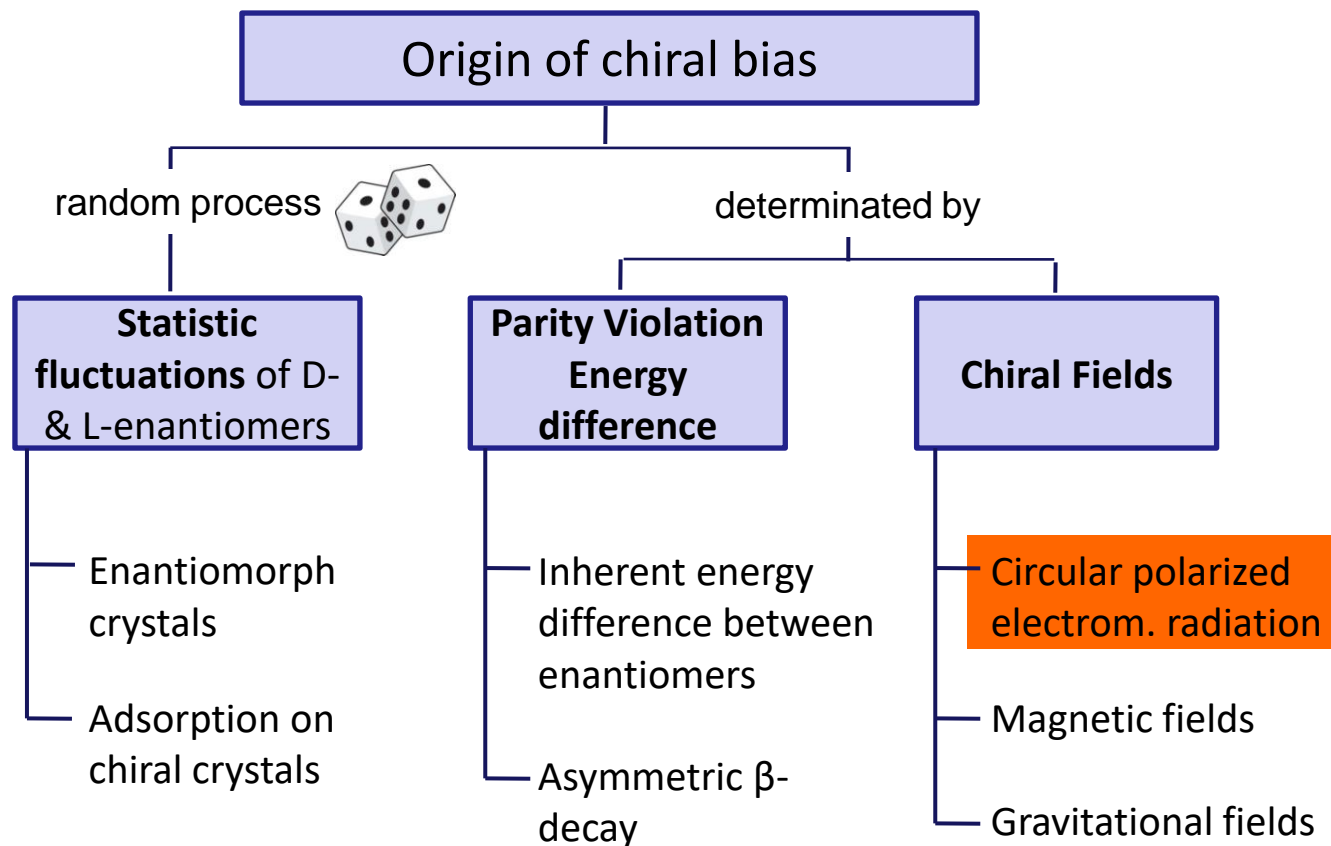
Proteins

chiral
monomer



α -L-amino acids

Amino acids



Scheme 2: Theories for an abiogenic origin of life's L-enantiomeric excess leading to homochirality on early Earth.

Evans, Meinert et al. *Chem. Soc. Rev.* **41** (2012), 5447–5458
Meinert et al. *Phys. Life Rev.* **8** (2011), 307–330
Meinert et al. *Symmetry* **2** (2010), 1055–1080

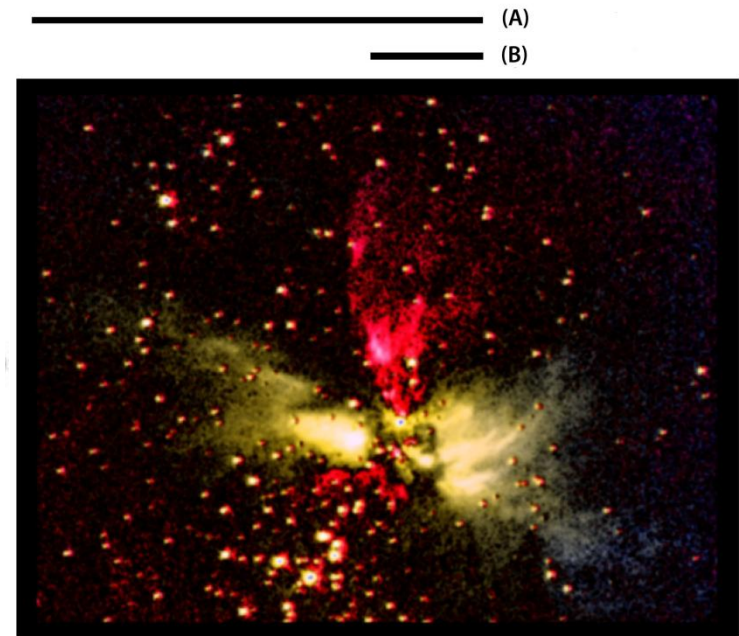
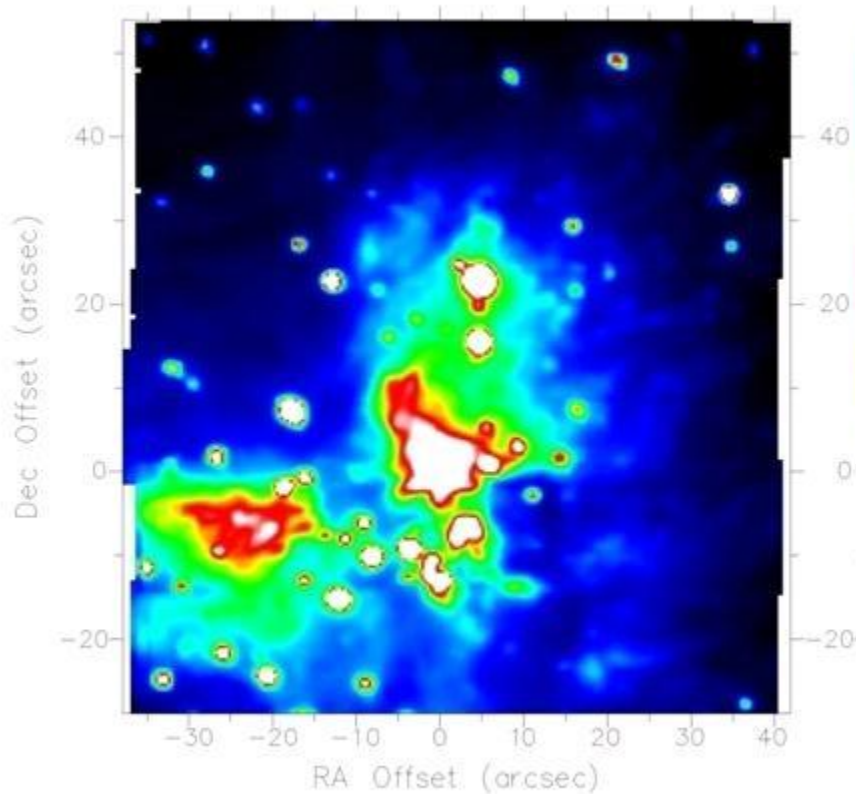
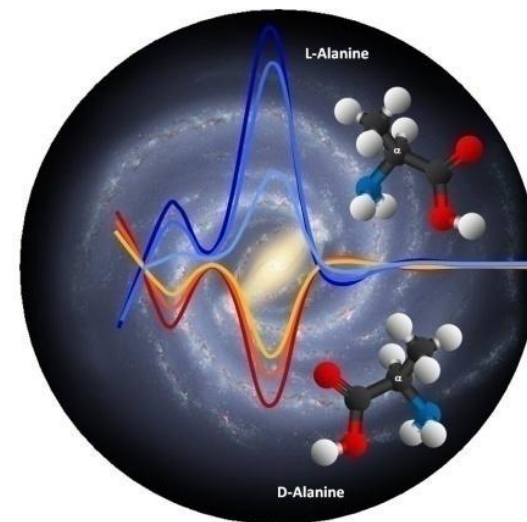
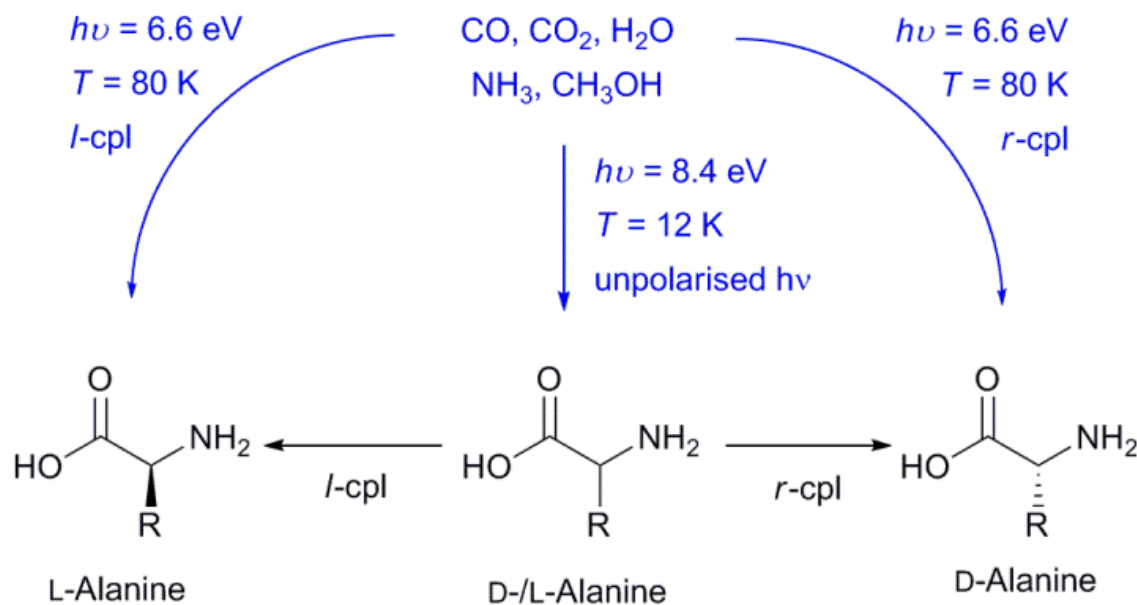


Image provided by the National Astronomical Observatory of Japan (SIPROL telescope, 2010)

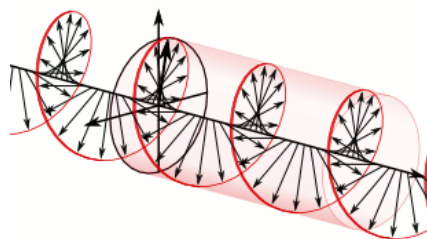
Fig. 24: Circular polarization image of the OMC-1 star formation region at 2.2 μm . (Left) Percentage of circular polarization ranging from -5% (black) to $+17\%$ (white). (Right) This image was captured using SIRPOL, the SIRIUS camera's mode of measuring circular polarity (IR). Yellow color expresses left-handed circular polarization. Red color expresses right-handed circular polarization. (A) expresses ~ 400 times the size of the solar system, and (B) shows ~ 100 times the size of the Solar System.

OMC-1: Bailey et al. *Science* **281** (1998), 672–674; Fukue et al.: *OLEB* **40** (2010), 335–346.

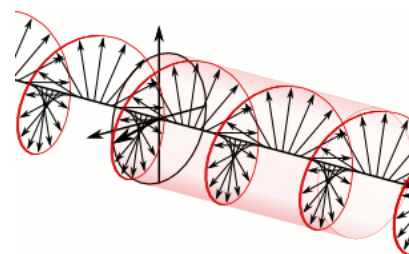
NGC 6334: Kwon et al.: *ApJL* **765** (2013), L6.



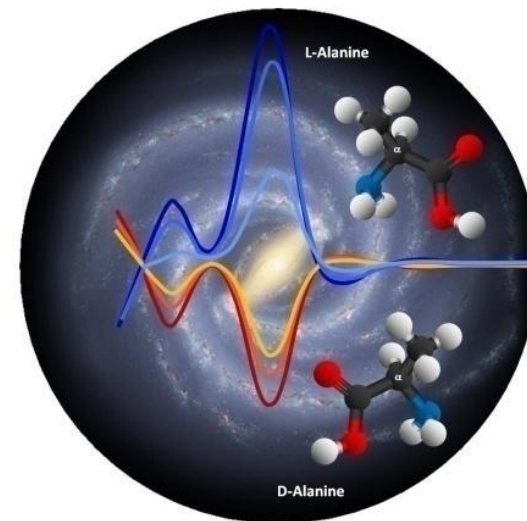
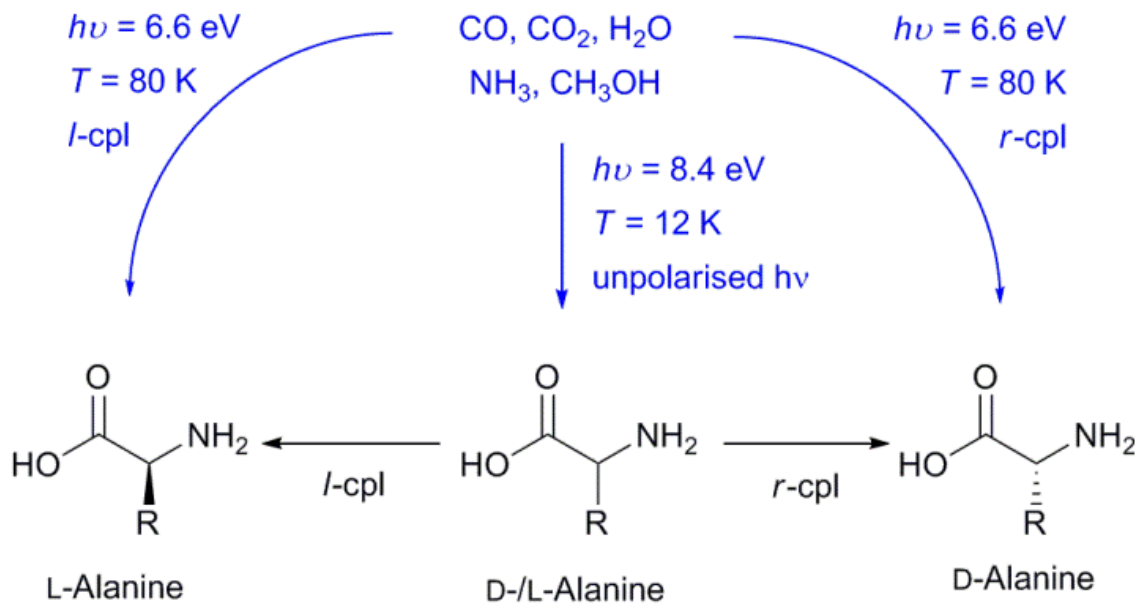
Scheme 3: Asymmetric photochemistry with circularly polarized light (CPL).



Left circularly polarized light



Right circularly polarized light



Scheme 3: Asymmetric photochemistry with circularly polarized light (CPL).

Enantiospecific photochemistry depends on:

$$\Delta\epsilon = \epsilon_R - \epsilon_L$$

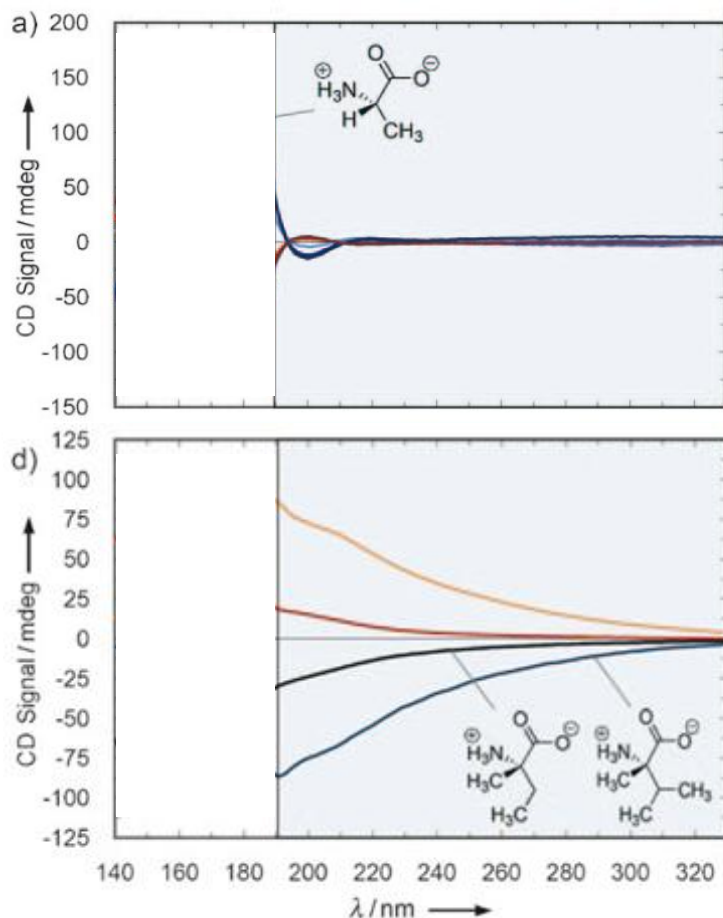
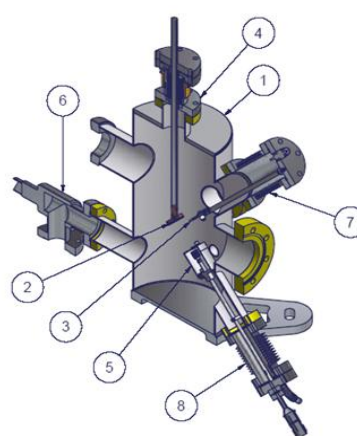


Fig. 26: CD spectra of isotropic amorphous amino acid films between 140 and 190 nm. a) Blue lines: L-alanine; red lines: D-alanine. b) L-isovaline (black), D-isovaline (red), L- α -methyl valine (blue), D- α -methyl valine (orange).



A

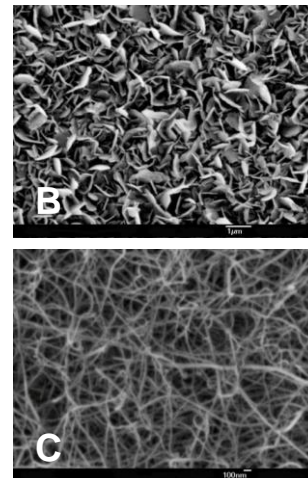
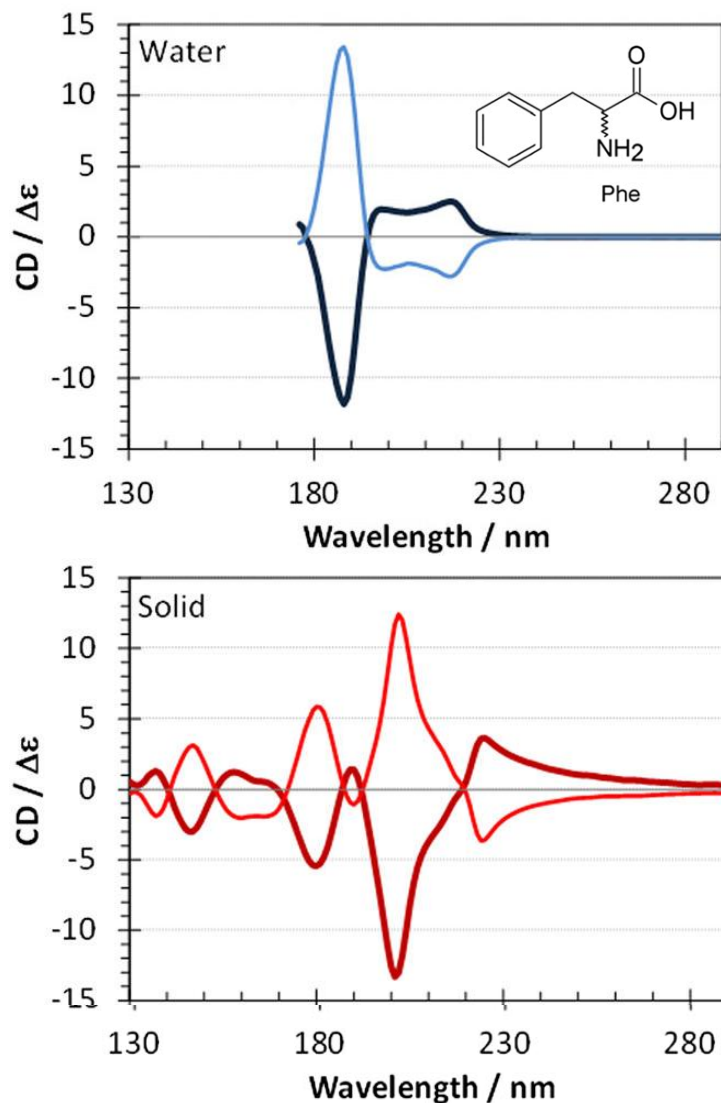


Fig. 27: Temperature- and pressure-controlled UHV chamber for controlled sublimation of amino acids (A). Scanning electron microscope (SEM) images of isotropic amorphous L-valine and (B) D- α -methyl valine (C). The non-crystalline **isotropic amorphous films show no long-range order.**

Meierhenrich, MEINERT et al. *Angew. Chem. Int. Ed.* **49** (2010), 7799–7802.



$$g(\lambda) = 4R/D = \Delta\epsilon/\epsilon$$

W. Kuhn *Naturwissenschaften* 17 (1929), 227.

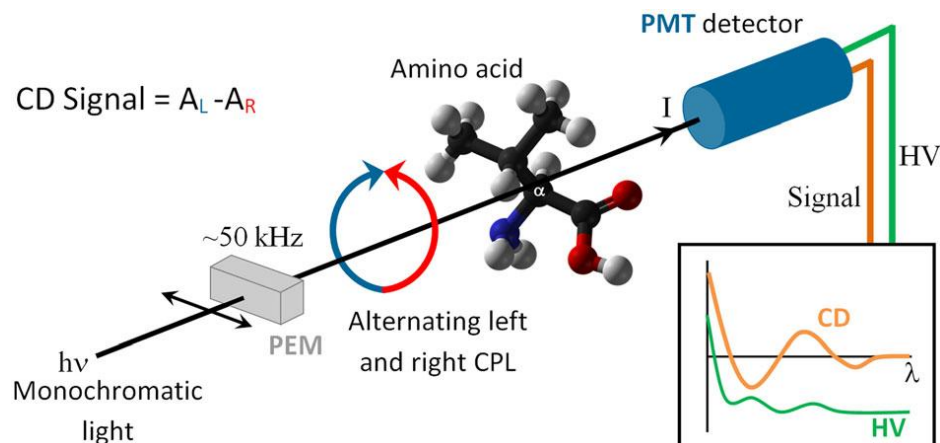
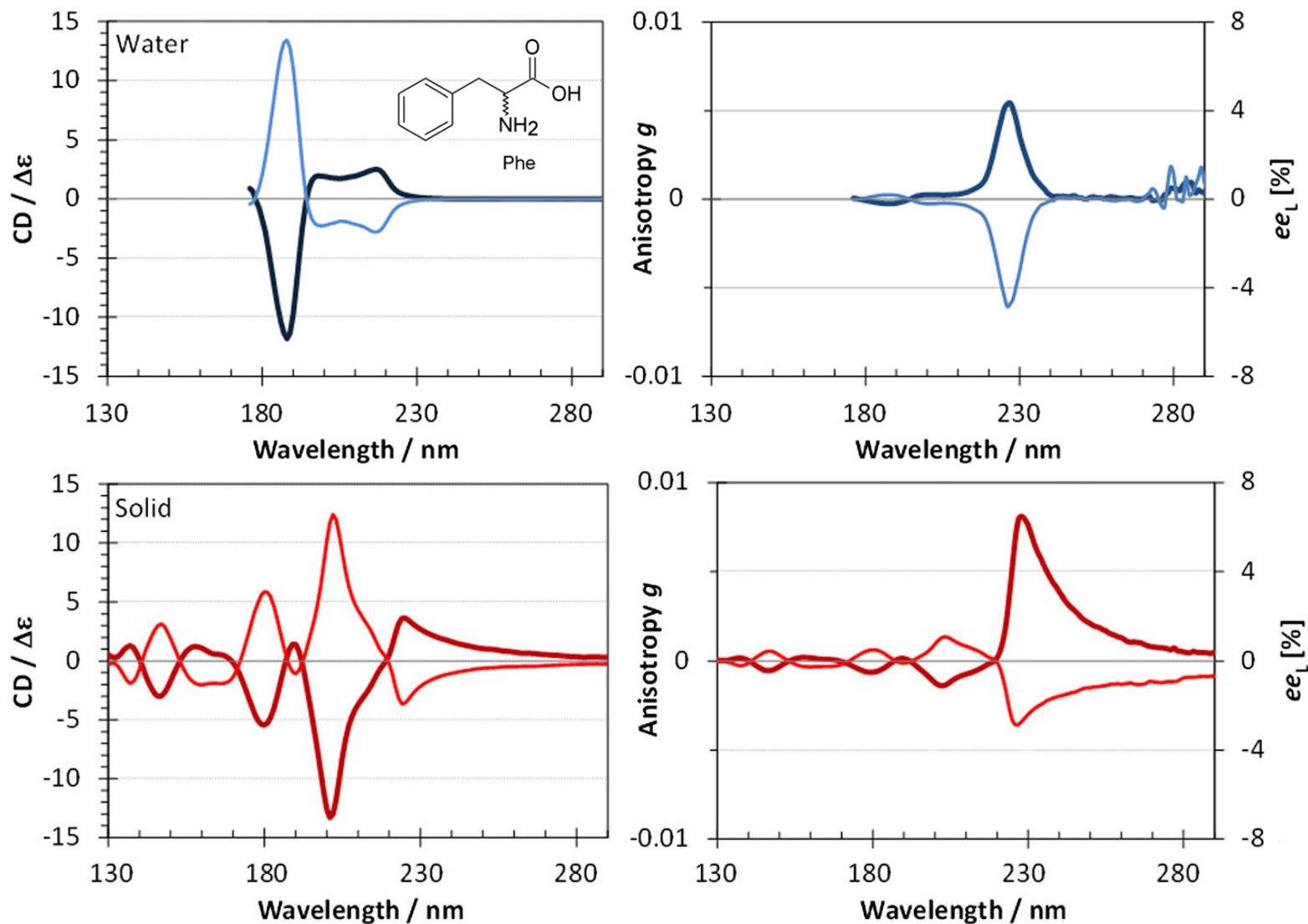


Fig. 28: Experimental set-up for recording anisotropy spectra in the VUV spectral range using a synchrotron radiation (SR) source. Both the differential absorption ΔA of alternating l- and r-CPL by optically active amino acid enantiomers and the sample absorbance A is recorded simultaneously to obtain anisotropy spectra $g(\lambda) = \Delta A/A$.

Evans, MEINERT et al. *Anisotropy spectra for chiral differentiation of biomolecular building blocks*. Topics in Current Chemistry. Ed. Cintas P, Springer, Berlin (2013)

FROM CIRCULAR DICHROISM SPECTROSCOPY TO ANISOTROPY SPECTROSCOPY



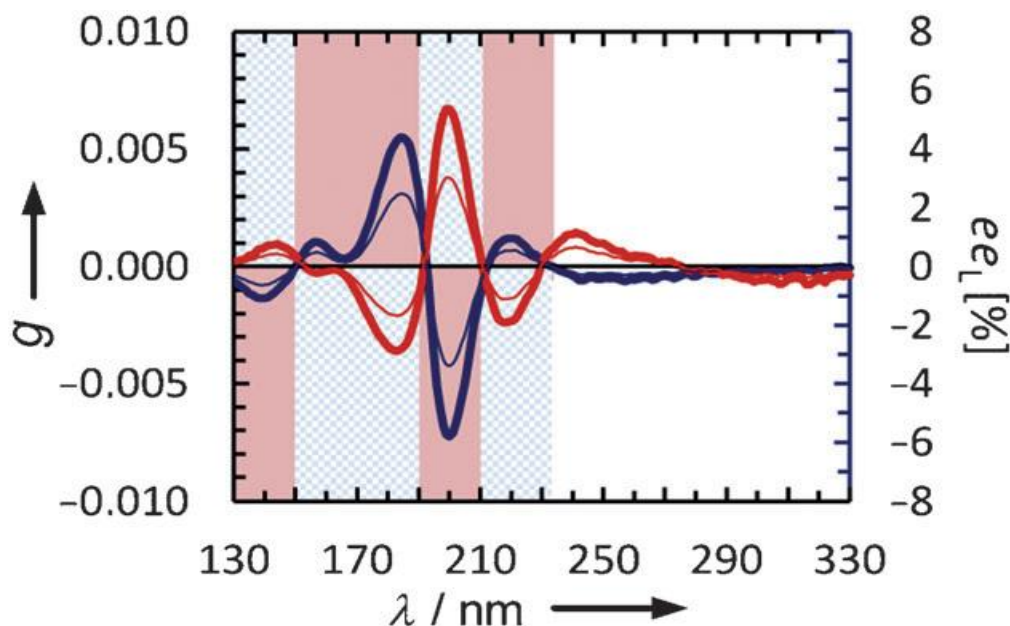


Fig. 29: Anisotropy spectra of isotropic amorphous D-alanine (red) and L-alanine (blue) in the vacuum UV and UV spectral region. Thin lines represent the L-enantiomeric excess (ee_L) inducible by either left- or right-cpl into alanine at a given photolysis rate of 99.99 %.

MEINERT et al. *Angew. Chem. Int. Ed.* **51** (2012), 4484–4487

$$g(\lambda) = 4R/D = \Delta\epsilon/\epsilon$$

$$ee \geq (1 - (1 - \xi)^{g/2}) \times 100 \%$$

- a) prediction of the sign of the induced ee ,
- b) determination of kinetics and ees of enantioselective photolysis,
- c) the selection of the CPL wavelength best suited for inducing ee .

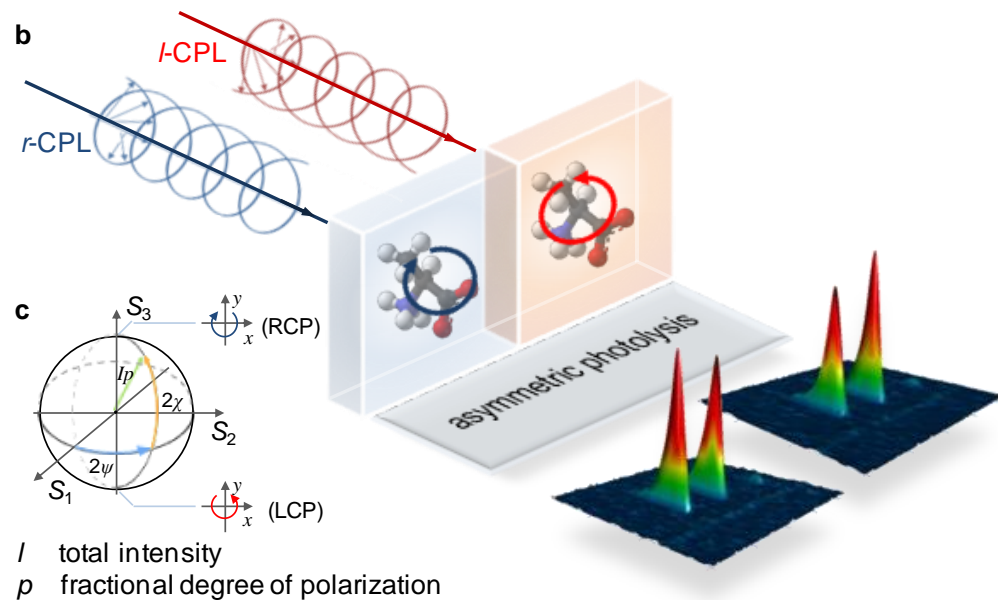
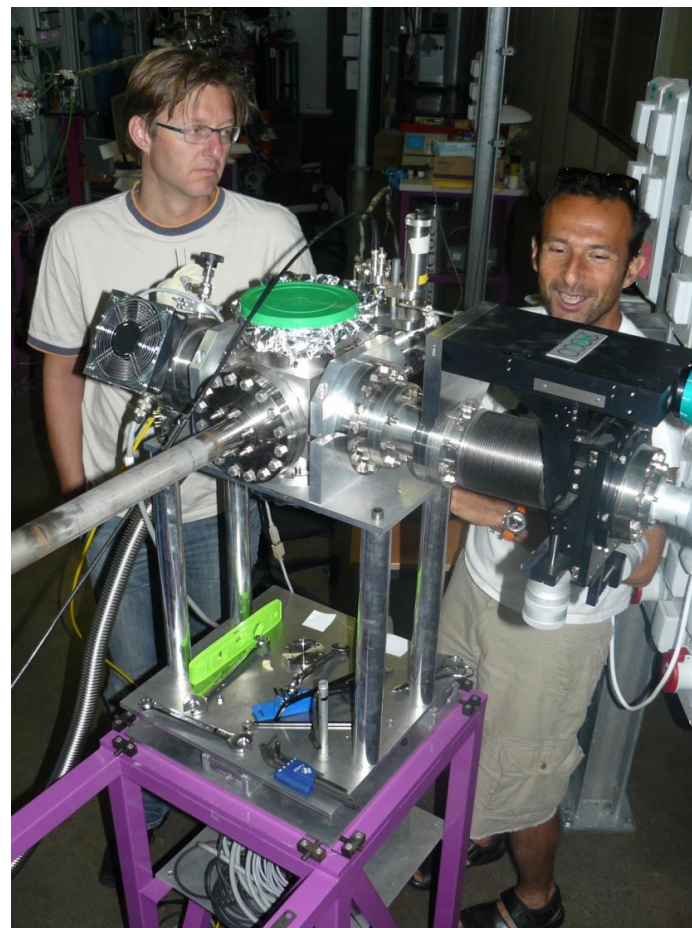


Fig. 30: Schematic outline of energy-tunable asymmetric photolysis. **b**, Photolytic induction of ee into amino acids as a function of CPL energy and circular polarization. Energy-tunable and tailored elliptical polarization as defined by its Stokes parameters (S_1 , S_2 , and S_3 , **c**) are provided by the HU640 undulator at the DESIRS beamline on the SOLEIL storage ring.



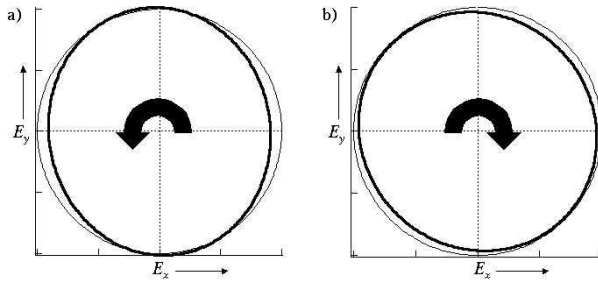


Fig. 31: Measured polarization ellipses (thick lines) at the sample location as produced by the OPHELIE2, HU640 type undulator. Absolute circular polarization rates are of 91 % for r-CPSR (b) and 94 % for l-CPSR (a).

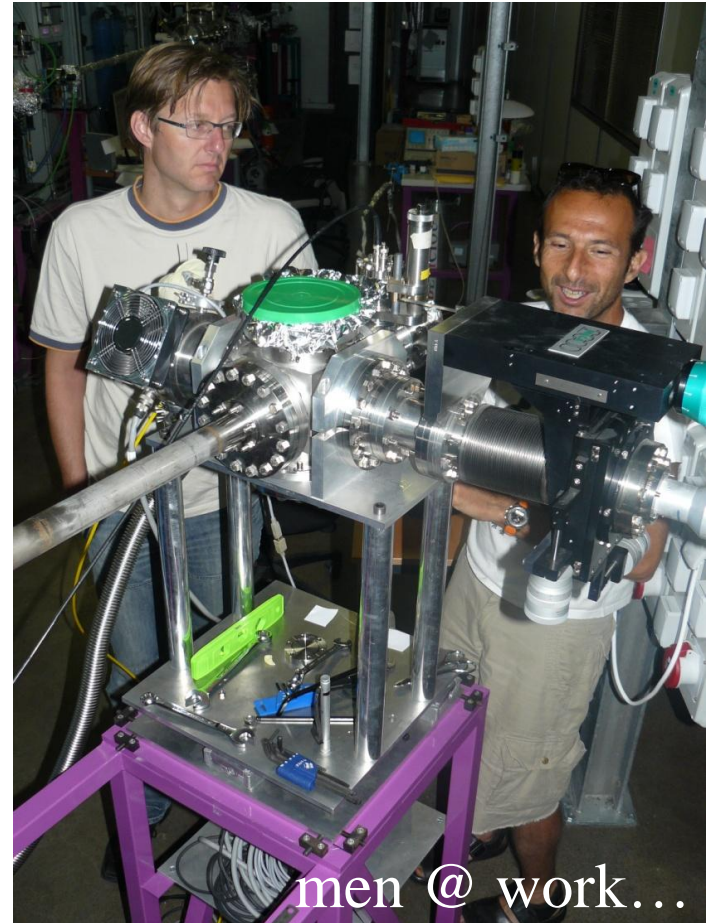


Fig. 32: The synchrotron SOLEIL is a third generation synchrotron optimized for intense photon fluxes. It started its activities in December 2006.



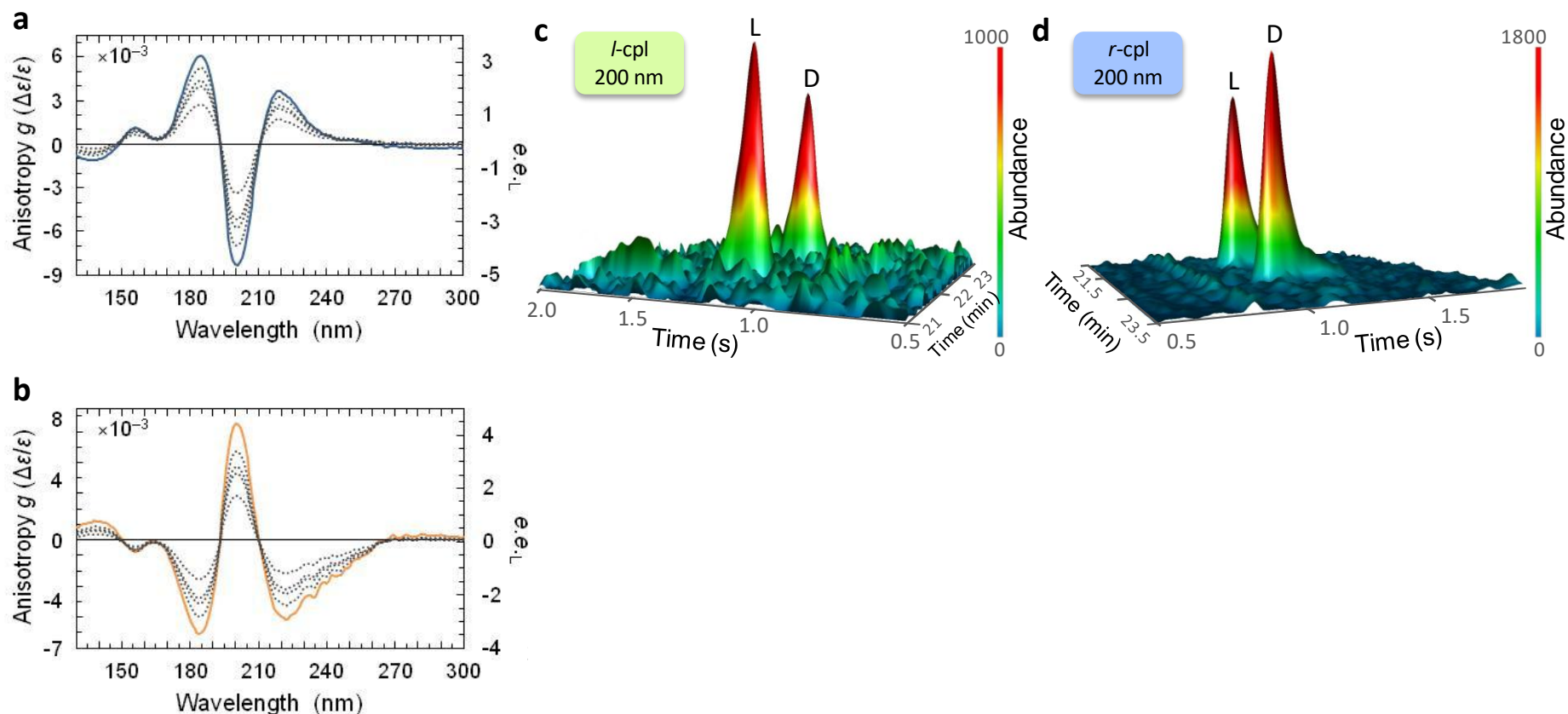


Fig. 33: Energy- and polarization-dependent CPL-induced symmetry breaking. (a, b) Anisotropy spectra $g(\lambda)$ and inducible ee_L of L-Ala & D-Ala. (c–d) Enantioselective GC×GC of ^{13}C -Ala after irradiation with different CPL-polarization and at different photon energies for 5h.

➤ UV CPL forms enantiomer-enriched amino acids

➤ sign of induced ee depends upon helicity of CPL

➤ sign of induced ee depends upon the energy of l -CPL and r -CPL

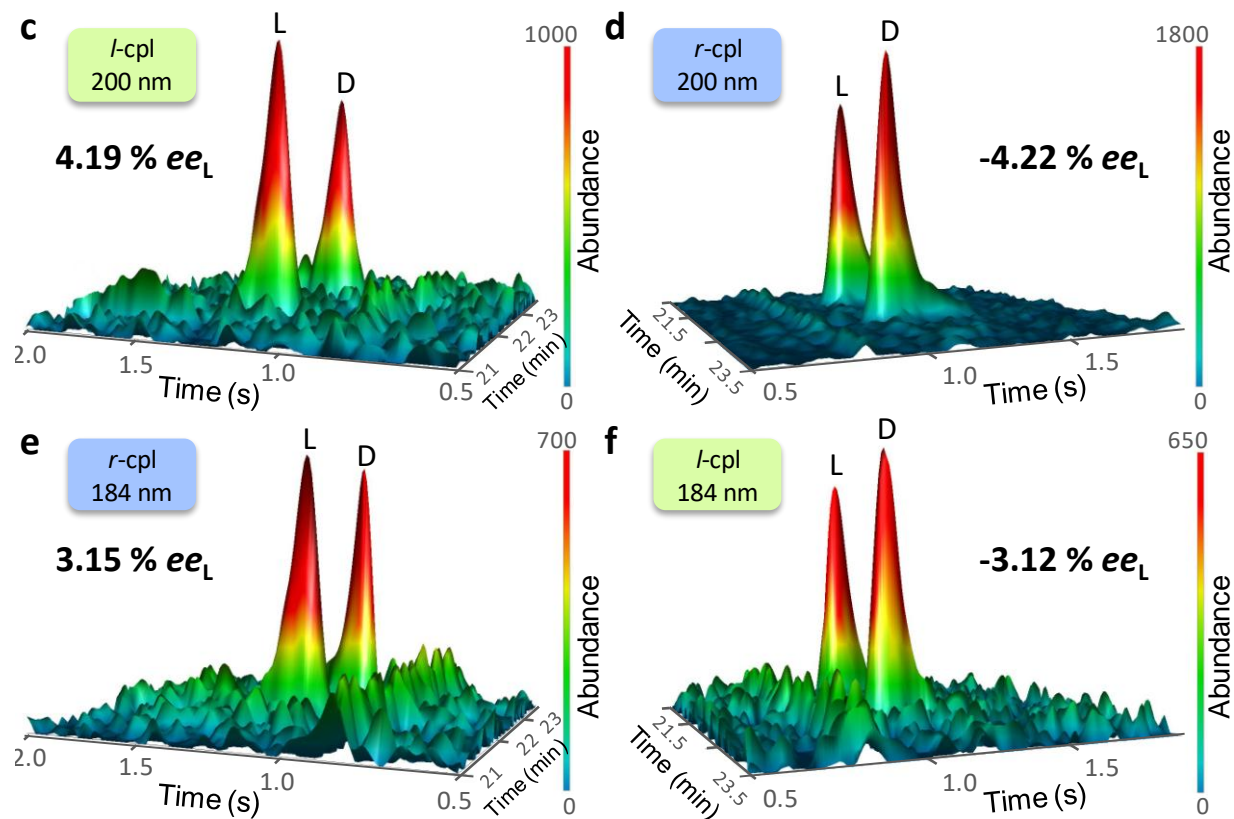


Fig. 34: Energy- and polarization-dependent CPL-induced symmetry breaking. (a, b) Anisotropy spectra $g(\lambda)$ and inducible ee_L of L-Ala & D-Ala. (c–d) Enantioselective GCxGC of ^{13}C -Ala after irradiation with different CPL-polarization and at different photon energies for 5h.

ABSOLUTE ASYMMETRIC AMINO ACID SYNTHESIS

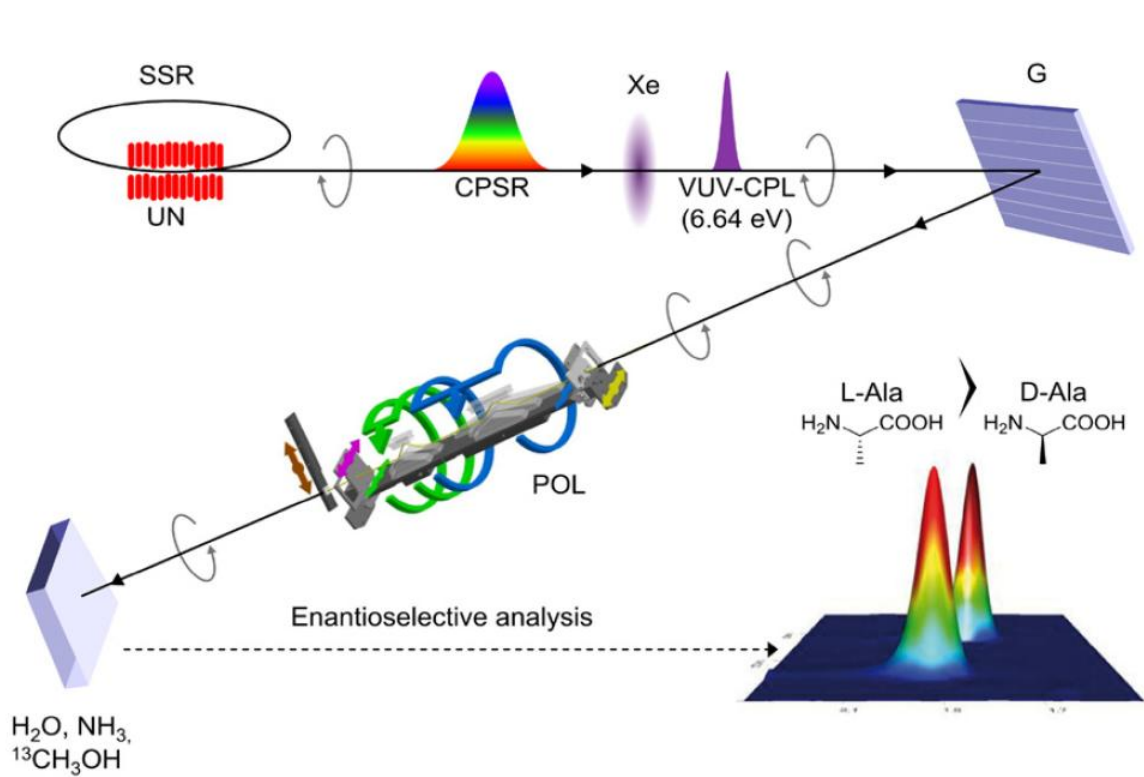
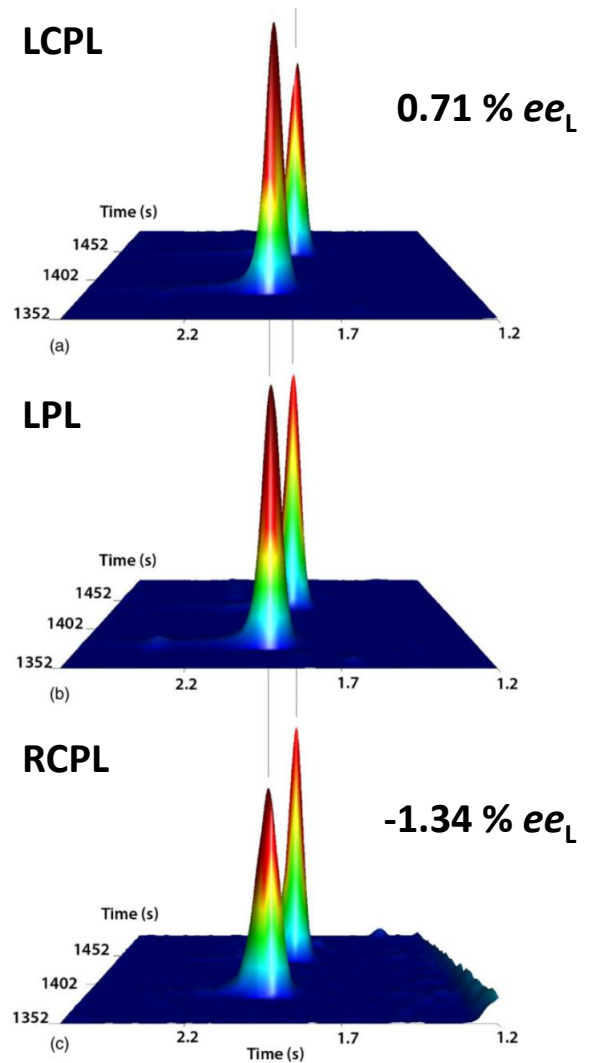


Fig. 35: Set-up of asymmetric VUV photolysis at the synchrotron radiation facility SOLEIL (left). Multidimensional gas chromatograms of ^{13}C -alanine enantiomers for the three polarization regimes (right).

DE MARCELLUS, MEINERT et al. *Astroph. J. Letters* **727** (2011), L27



ASYMMETRY INDUCED IN EXTRATERRESTRIAL ICE ANALOGUES

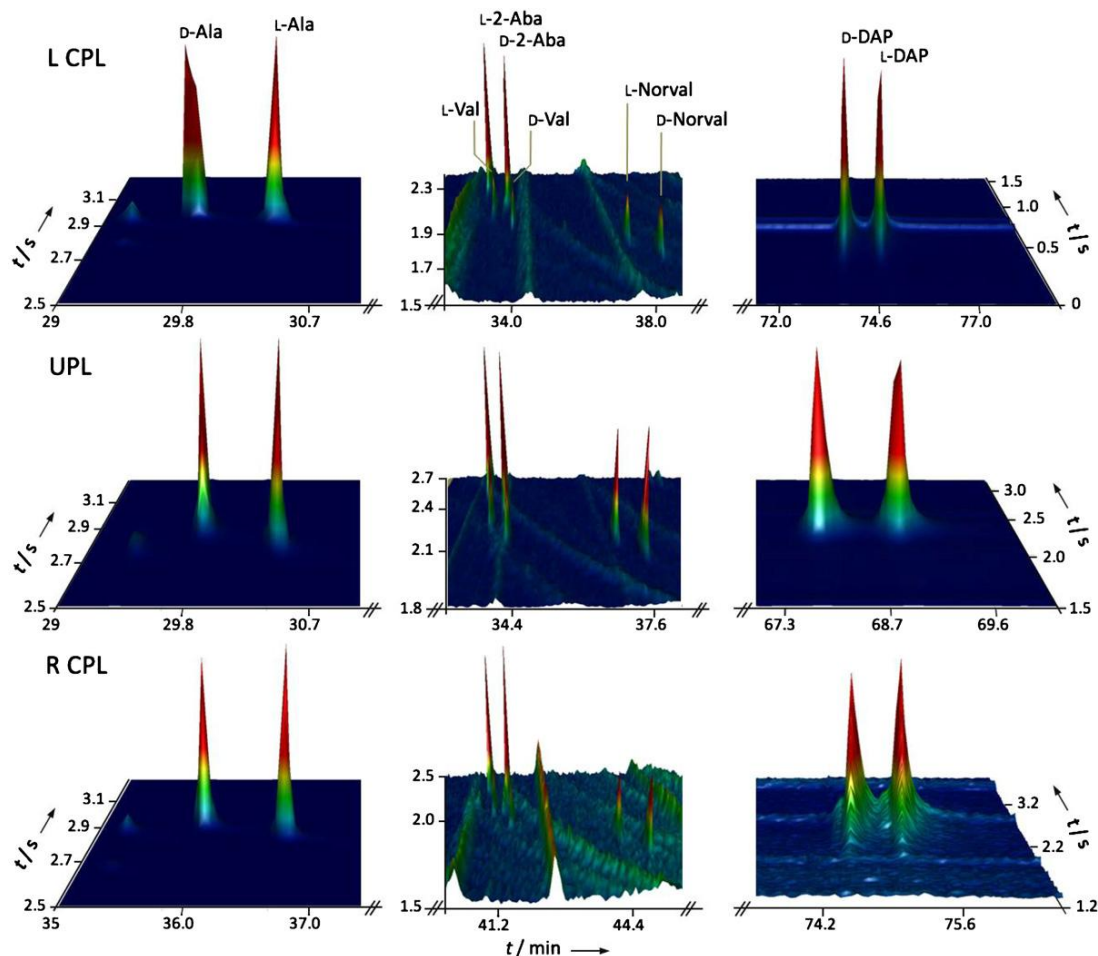


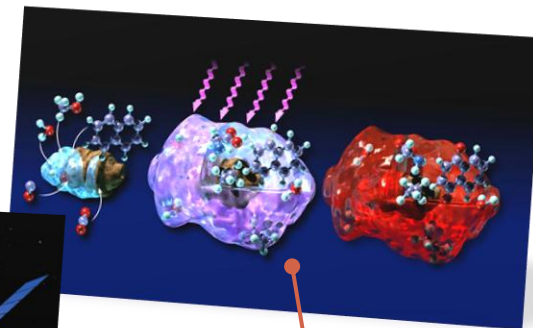
Fig. 36: Multidimensional enantioselective GC resolution of ^{13}C enantiomers of alanine (Ala), 2-aminobutyric acid (2-Aba), valine (Val), norvaline (Norval), and 2,3-diaminopropionic acid (DAP) produced by 10.2 eV UV photoirradiation with (a) L CPL, (b) UPL, and (c) R CPL.

Table 2 | Enantiomeric excesses ee_L induced *via* asymmetric photolysis/synthesis into achiral interstellar ice analogues at photon energy 10.2 eV.

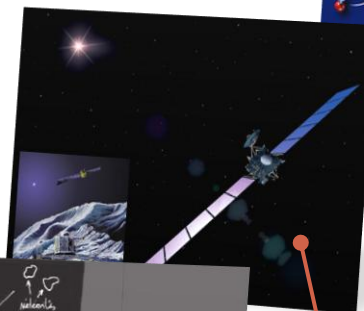
Amino acid	<i>l</i> -CPL ee_L [%]	<i>r</i> -CPL ee_L [%]
α -Alanine	-0.34 ± 0.24	1.04 ± 0.39
2-Aminobutyric acid	-2.54 ± 0.28	1.28 ± 0.22
Valine	-1.82 ± 0.30	1.08
Norvaline	-0.78 ± 0.39	0.90 ± 0.33
2,3-Diaminopropionic acid	-0.20 ± 0.14	2.06 ± 0.34

- UV CPL forms enantiomer-enriched amino acids
- sign of induced ee is identical for all amino acids for a given helicity
- sign of induced ee depends upon the energy of *l*-CPL and *r*-CPL

We are made of stardust...



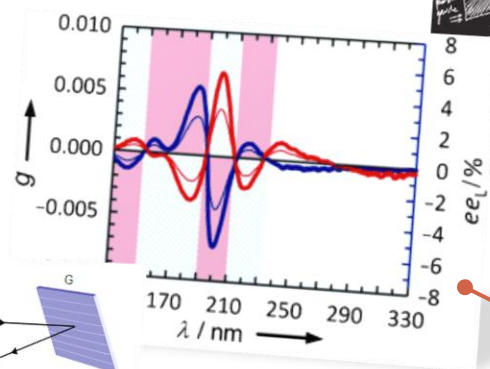
(1) **Interstellar Ice Chemistry:** laboratory produced ice *photo*-chemistry under controlled astrophysical conditions



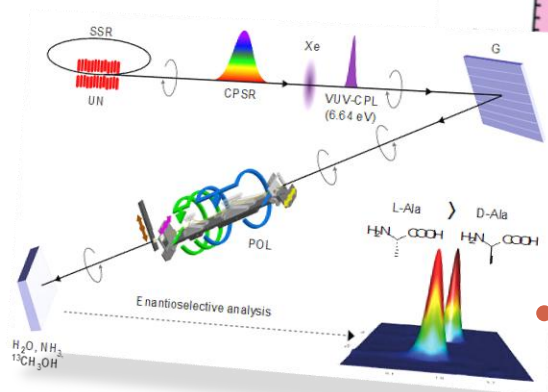
(2) **ROSETTA** – International mission to a comet, in search of life's biomolecular origins



(3) Life requires **Homochirality** in certain biomolecules



(4) **Anisotropy spectra** to study the chiroptical properties of biomolecules



(5) **Enantioselective photolysis & photosynthesis**

WHAT TO DO NEXT ?

- **Asymmetric photolysis:** tuning energy-selective photolysis of ribose and sugar precursor structures to understand the asymmetry of the genetic material
- **Absolute asymmetric synthesis:** ice simulation experiments using UV-CPL to form *in-situ* enantioenriched aldehydes, sugars, and amino acids
- **Cross-linked interpretation with** carbonaceous chondrites / micrometeorites / ExoMars, Hayabusa 2, OSIRIS Rex ...

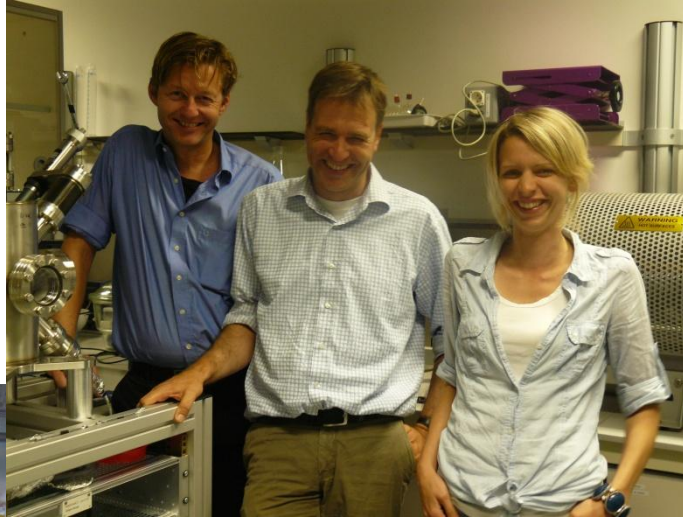
Some questions to ponder:

How might enantioenrichment have been (autocatalytically) amplified and maintained in aqueous, racemizing environments ?

Is homochirality a requirement for life or a result of it?

What might have been the requirements for the first biopolymers & what molecules can fulfill these requirements?

MERCI à mes collègues



...best "LabFriend"



Acknowledgements

Pr. U.J. MEIERHENRICH **Université de Nice Sophia Antipolis**

Dr. L. NAHON **Synchrotron SOLEIL**

Dr. S. HOFFMANN **Institute for Storage Ring Facilities, Aarhus**

Dr. N. JONES **Institute for Storage Ring Facilities, Aarhus**

Dr. L. d'HENDECOURT **Institut d'Astrophysique Spatiale, Paris**

Dr. G. DANGER **PIIM – Université Aix & Marseille**

Dr. M. VISO **CNES, Paris**

Dr. Z. Martins **Imperial College London**



Appendix

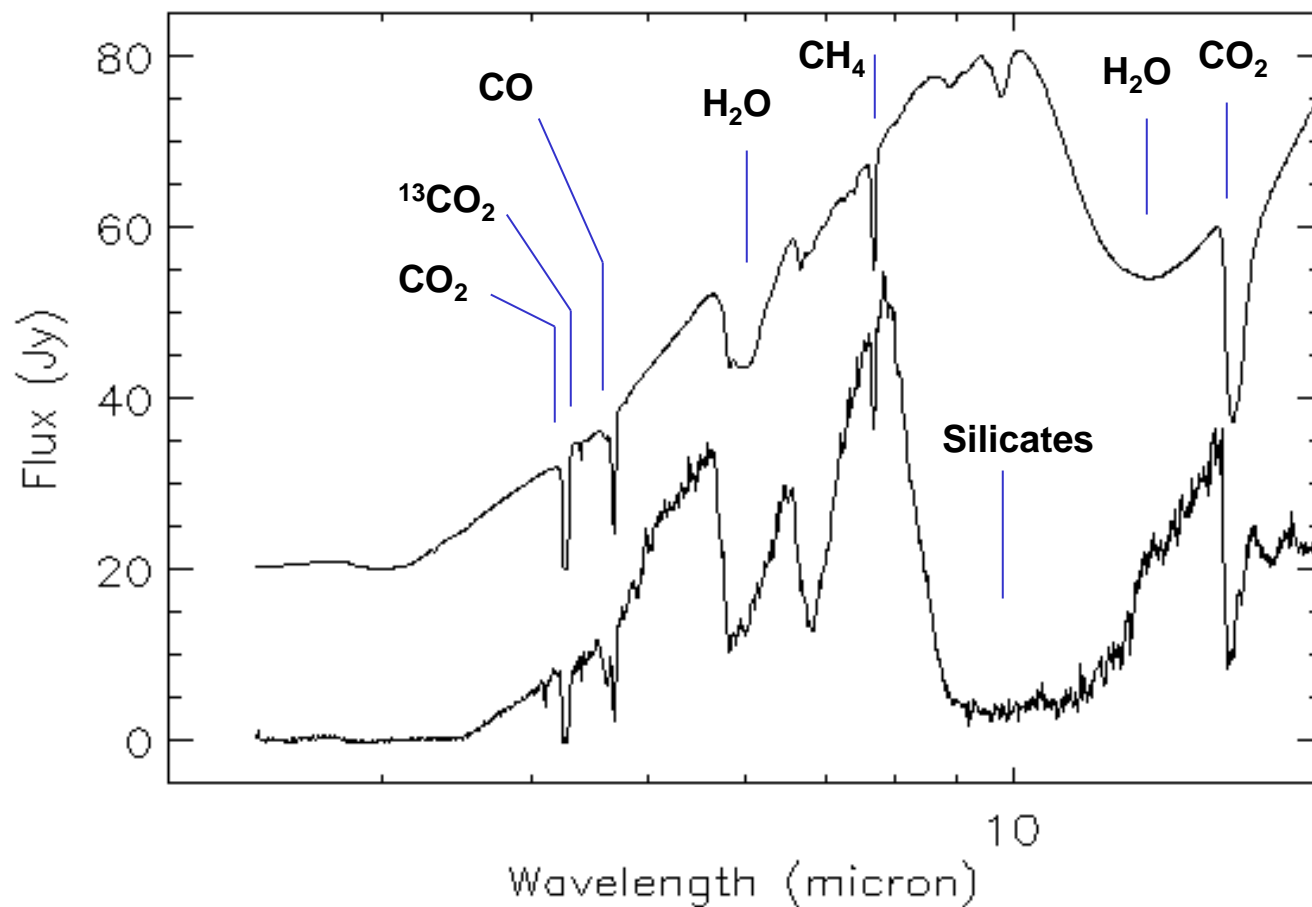


Fig. A-1: ISO SWS (S01) spectrum of the source RAFGL 7009S between 2.5 and 18 microns (bottom), compared with a laboratory spectrum of a photolysed ice mixture $\text{H}_2\text{O}:\text{CO}:\text{CH}_4:\text{NH}_3:\text{O}_2 = 10:2:1:1:1$ (top).

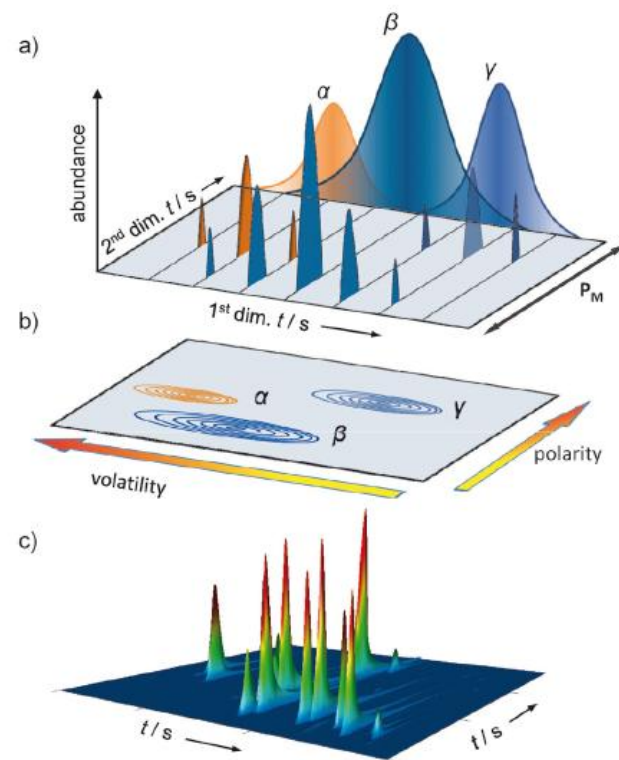
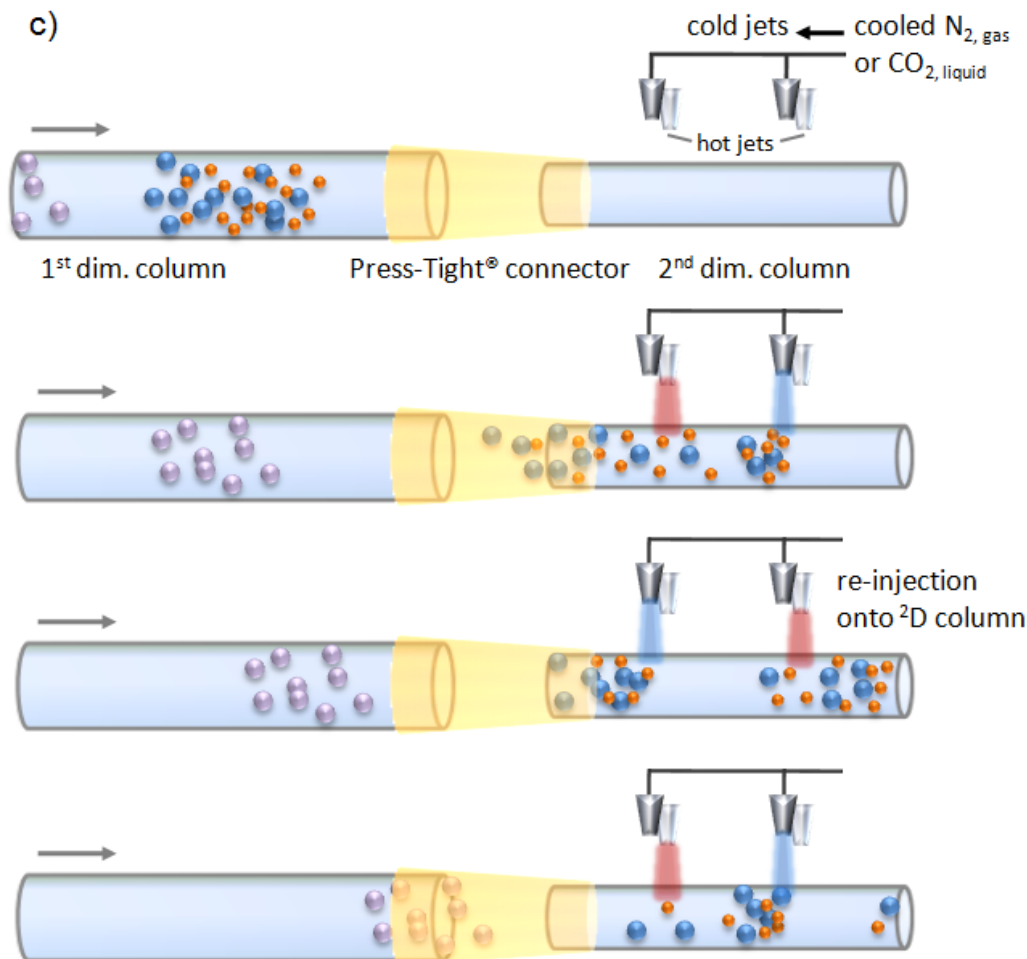
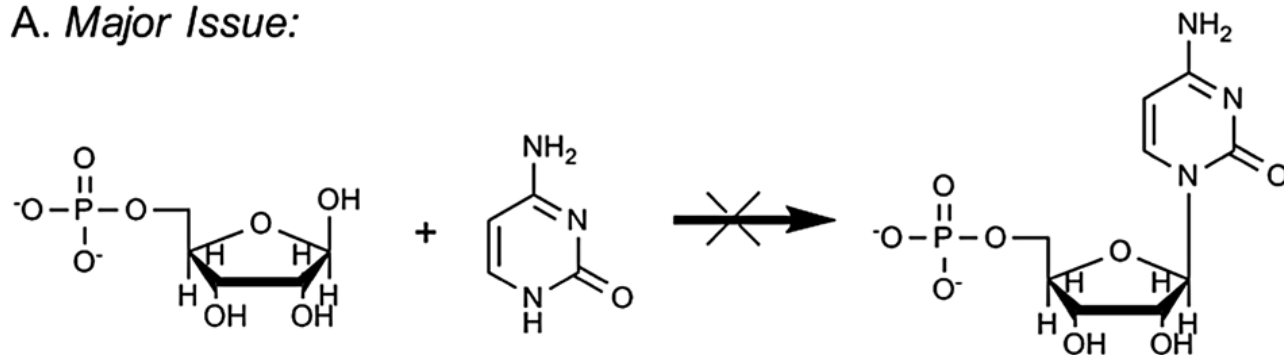
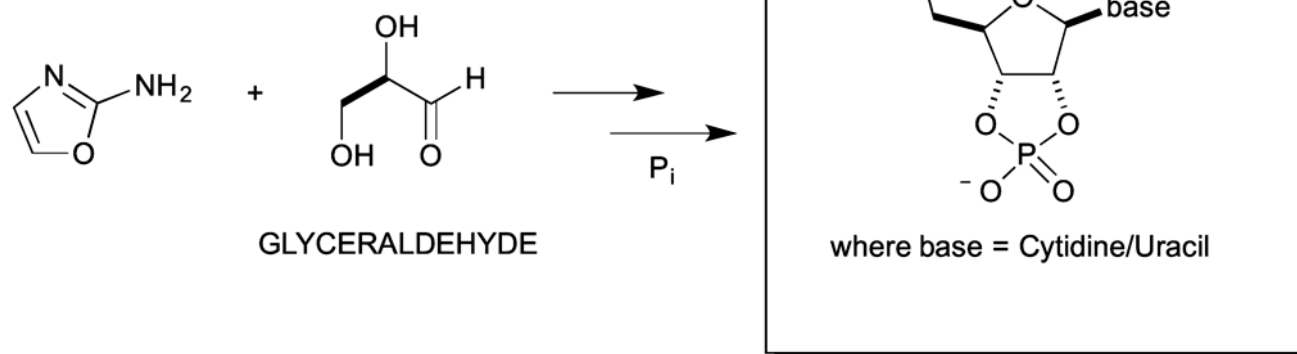


Figure 1. Illustration of a GC × GC chromatogram. a) Chromatographic peaks (α , β , and γ) eluted from a typical apolar 1^D column sequentially sliced into distinct fractions during a defined modulation period (P_M). Non-resolved analytes are often better resolved on a (generally polar) short micro-bore 2^D column. b) The data stream from the detector is then plotted based on the modulation in a 2D contour color plot format or c) directly showing signal intensities in 3D presentation as conical peaks.

A. Major Issue:



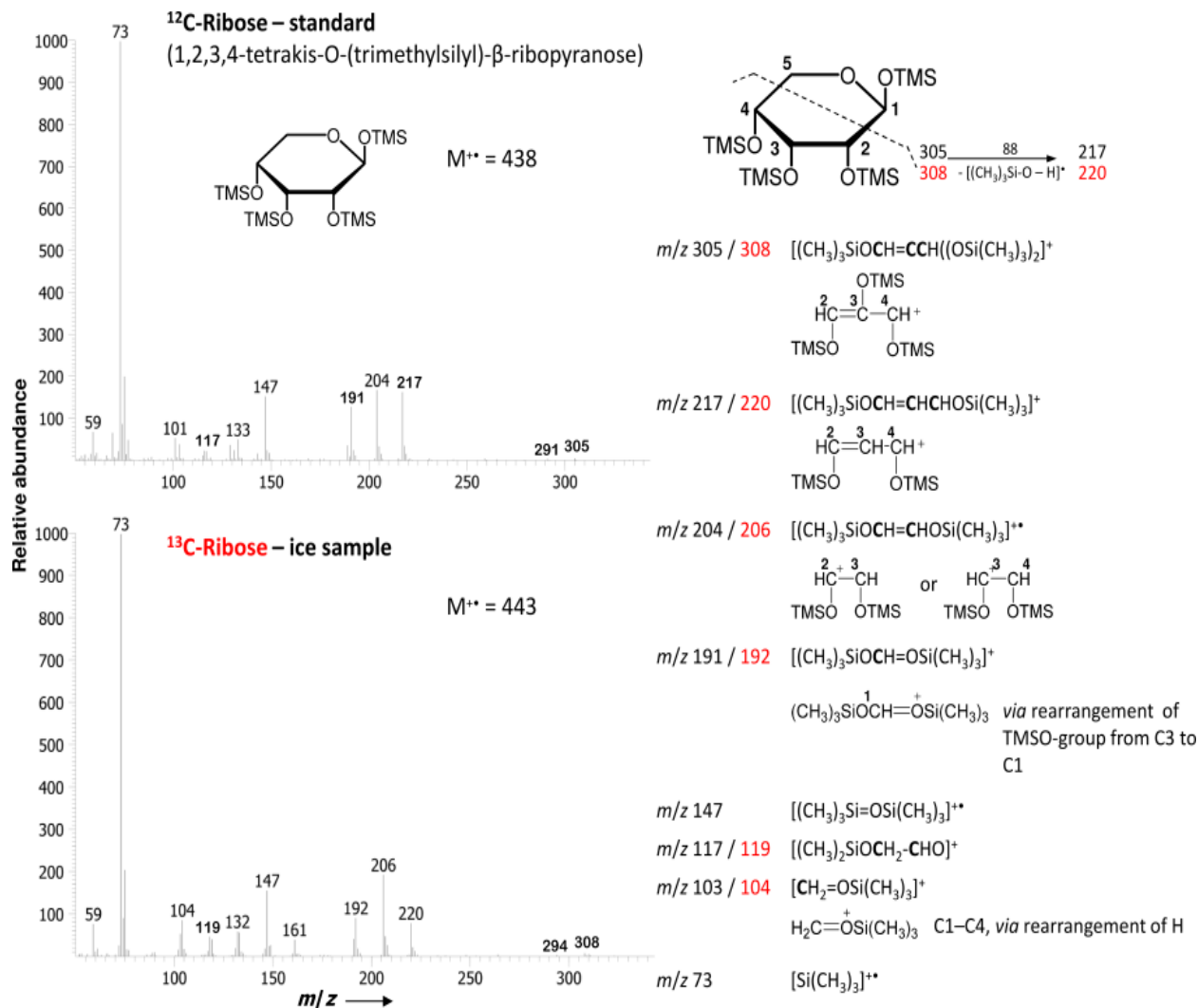
B. Alternative Synthetic Solution:



Scheme 1: (A) The RNA World is thermodynamically unfavourable if originating from ribose sugar plus nucleobase; (B) an alternative route to an RNA World.

Sutherland et al. *Nature* **459** (2009), 239–242

RIBOSE DETECTED IN COMETARY ANALOGUES



THE SIXTEEN MOLECULES USED TO FIT THE COSAC MASS SPECTRUM

Name	Formula	Molar mass [u]	MS fraction	Relative to water
Water	H ₂ O	18	80.92	100
Methane	CH ₄	16	0.70	0.5
Methanenitrile (Hydrogen cyanide)	HCN	27	1.06	0.9
Carbon monoxide	CO	28	1.09	1.2
Methylamine	CH ₃ NH ₂	31	1.19	0.6
Ethanenitrile (Acetonitrile)	CH ₃ CN	41	0.55	0.3
Isocyanic acid	HNCO	43	0.47	0.3
Ethanal (Acetaldehyde)	CH ₃ CHO	44	1.01	0.5
Methanamide (Formamide)	HCONH ₂	45	3.73	1.8
Ethylamine	C ₂ H ₅ NH ₂	45	0.72	0.3
Isocyanomethane (Methyl isocyanate)	CH ₃ NCO	57	3.13	1.3
Propanone (Acetone)	CH ₃ COCH ₃	58	1.02	0.3
Propanal (Propionaldehyde)	C ₂ H ₅ CHO	58	0.44	0.1
Ethanamide (Acetamide)	CH ₃ CONH ₂	59	2.20	0.7
2-Hydroxyethanal (Glycolaldehyde)	CH ₂ OHCHO	60	0.98	0.4
1,2-Ethanediol (Ethylene glycol)	CH ₂ (OH)CH ₂ (OH)	62	0.79	0.2

Goesmann et al., *Science* **349** (2015), aab0689

COSAC EXPERIMENT ONBOARD ROSETTA - IN SEARCH OF LIFE'S MOLECULAR ORIGINS

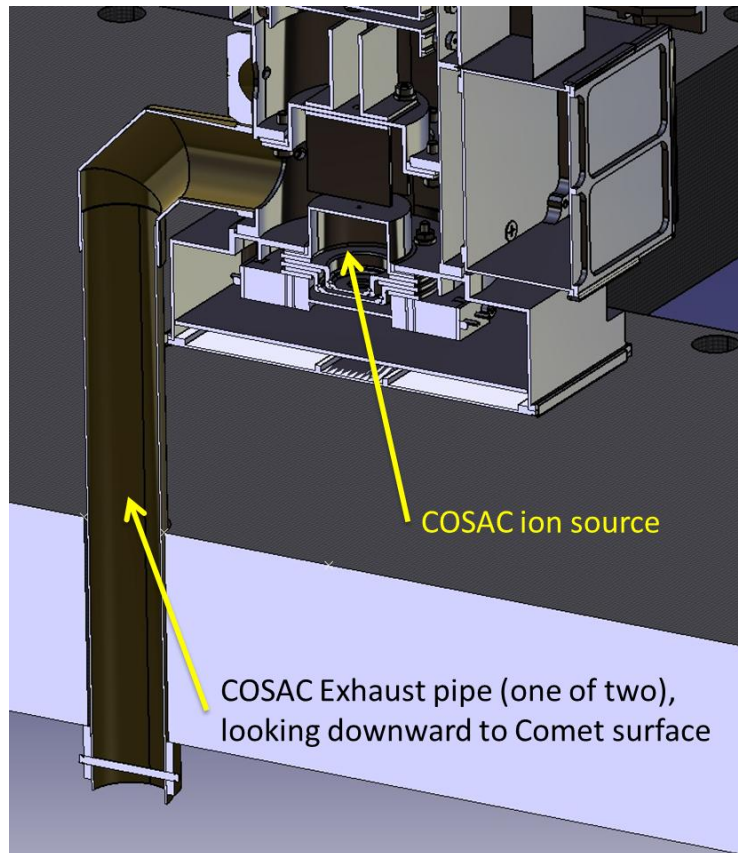


Fig. 22: Cross section of the COSAC exhaust; the image shows one of the exhaust tubes in cross section (19 mm inner diameter) where cometary dust could have entered.



Goesmann, Meierhenrich et al., *Science* **349** (2015), aab0689

MASS SPECTRA TAKEN BY COSAC IN MS-ONLY MODE

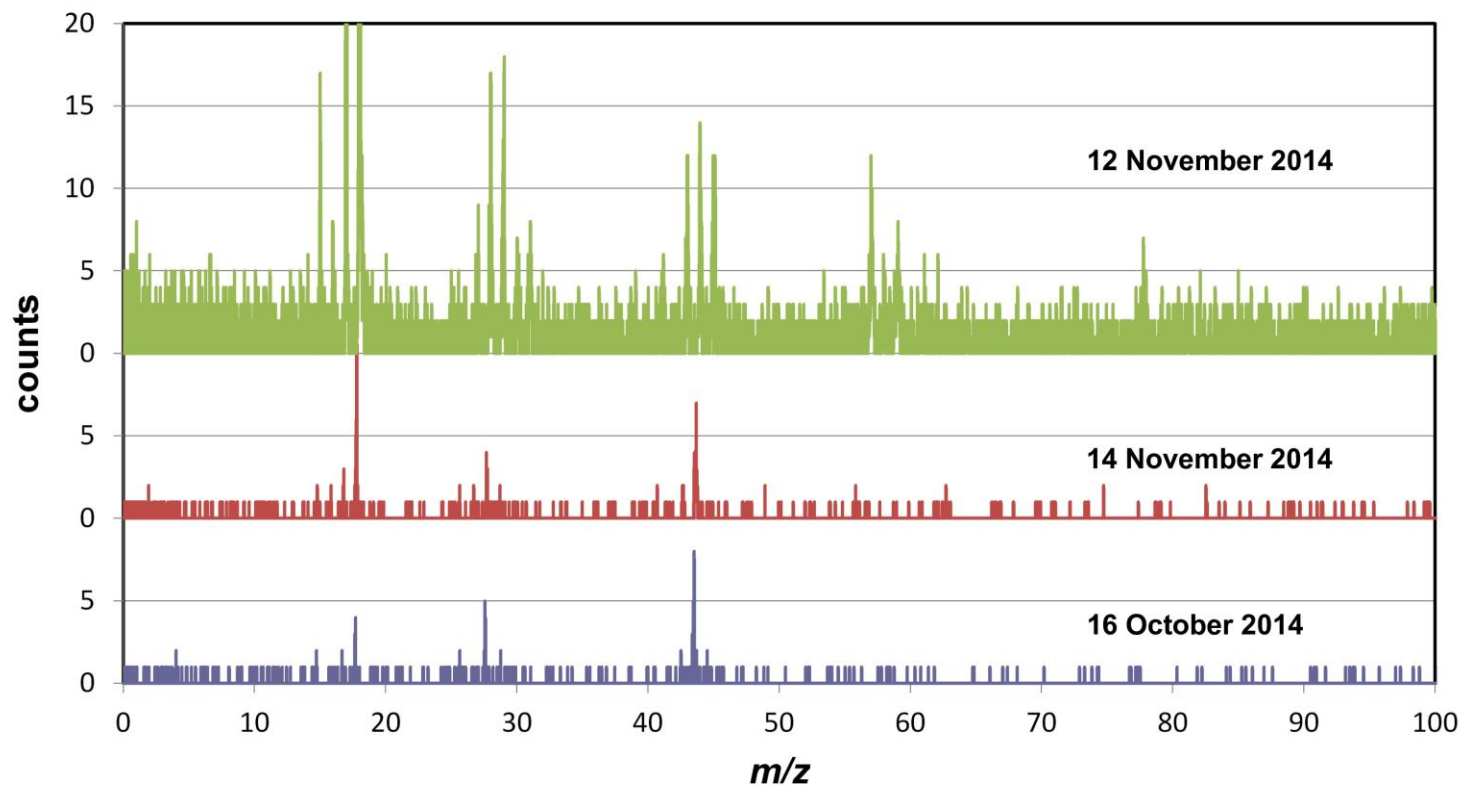


Fig. 23: Top (green): spectrum taken 25 minutes after first touchdown; the m/z 18 peak reached a height of 330 counts, but the spectrum is truncated to show smaller peaks more clearly; middle (red): final spectrum, taken two days later at the current Philae position; bottom (blue) first spectrum, obtained in orbit 27 days prior to landing, from a distance of 10 km.

F. Goesmann et al., *Science* **349** (2015), aab0689.